

Green Chemistry

Accepted Manuscript



This is an *Accepted Manuscript*, which has been through the Royal Society of Chemistry peer review process and has been accepted for publication.

Accepted Manuscripts are published online shortly after acceptance, before technical editing, formatting and proof reading. Using this free service, authors can make their results available to the community, in citable form, before we publish the edited article. We will replace this *Accepted Manuscript* with the edited and formatted *Advance Article* as soon as it is available.

You can find more information about *Accepted Manuscripts* in the [Information for Authors](#).

Please note that technical editing may introduce minor changes to the text and/or graphics, which may alter content. The journal's standard [Terms & Conditions](#) and the [Ethical guidelines](#) still apply. In no event shall the Royal Society of Chemistry be held responsible for any errors or omissions in this *Accepted Manuscript* or any consequences arising from the use of any information it contains.



www.rsc.org/greenchem

Combining Bio- and Chemo-Catalysis for the Conversion of Bio-Renewable Alcohols: Homogeneous Iridium Catalysed Hydrogen Transfer Initiated Dehydration of 1,3-Propanediol to Aldehydes

Yue-Ming Wang,^{a,b} Fabio Lorenzini,^a Martin Rebros,^c Graham C. Saunders,^d and Andrew C. Marr.*^{a,b}

^a School of Chemistry and Chemical Engineering, Queen's University of Belfast, UK.

^b Queen's University Ionic Liquids Laboratories (QUILL), UK.

^c Institute of Biotechnology and Food Science, Faculty of Chemical and Food Technology, Slovak University of Technology, Bratislava, Slovakia.

^d School of Science, The University of Waikato, Hamilton 3240, New Zealand.

**a.marr@qub.ac.uk*

Abstract.

Combining whole cell biocatalysis and chemocatalysis in a single reaction sequence avoids unnecessary separations, and the associated waste and energy consumption. Bacterial fermentation has been employed to convert waste glycerol from biodiesel production into 1,3-propanediol. This 1,3-propanediol can be extracted selectively from the aqueous fermentation broth using ionic liquids. 1,3-propanediol in ionic liquid solution was converted to propionaldehyde by hydrogen transfer initiated dehydration (HTID) catalysed by a Cp*IrCl₂(NHC) (Cp* = pentamethylcyclopentadienyl; NHC = carbene ligand) complex. The use of an ionic liquid solvent enabled the reaction to be performed under reduced pressure, facilitating the isolation of the product, and improving the reaction selectivity. The Ir(III) catalyst in ionic liquid was found to be highly recyclable.

Introduction.

The success of the oil and petrochemical industries can be attributed to the production of transportable fuels in parallel with the synthesis of chemicals, and in particular precursors to polymers and materials. Of the alternatives to fossil fuel energies, only biomass presents similar opportunities, and by analogy the production of biofuels is rendered more economical by coupling it to the production of chemicals from biomass, for example in a biorefinery. The conversion of food producing land to energy crops is understandably controversial, and should be avoided. More sustainable is the production of fuels from agricultural and food wastes. These wastes are ubiquitous, as all animals must eat, and therefore their utilisation provides real opportunities to develop low waste, highly sustainable industries. In Europe

used fats and oils are being upcycled into biodiesel in industrial plants on 100 thousand ton per annum scale. Biodiesel is a transportable bio-derived fuel, but production generates waste glycerol. This provides opportunities to introduce parallel chemicals production, but unfortunately the crude glycerol formed is a difficult substrate, as it is highly contaminated and very wet. The conversion of impure bio-renewable starting materials into valuable chemical products is a significant challenge.¹ Low cost starting materials available from biomass are, in general, very different from those derived from fossil fuels, and tend to be highly oxygenated, impure, aqueous, and dilute. These solutions of mixed aqueous oxygenates require purification from water and deoxygenation. This is in stark contrast to hydrocarbons, which require oxidation in their primary processing. As a result, the methods that have been developed for crude oil streams are not suitable for the treatment of biomass feeds, and a new generation of transformations and processes is required.

Whole cell biocatalysis provides a route by which crude biomass feeds can be mobilized. Bacteria, algae and fungi can be used to convert oxygenates at low concentration in impure aqueous solution into solutions rich in target chemicals.² A whole cell catalyst digests organic material and enriches the solution in the side-products of metabolism. Common products are alcohols and carboxylic acids. Coupling whole cell biocatalysis to downstream chemocatalytic transformations widens the variety of chemicals that can be prepared.³

1,3-propanediol (1,3-PDO) is a renewable platform chemical¹ that can be readily prepared by large scale whole cell biocatalysis.² Bio-derived 1,3-propanediol is currently produced by the bacterial fermentation of sugars.^{2,4} 1,3-PDO can be obtained at competitive cost and is commercially available from DuPont™ (marketed as Bio-PDO™).⁴

Although it is difficult to generate from biomass by chemical means, fermentative production of 1,3-PDO is relatively simple and environmentally friendly.⁵ 1,3-PDO is also a major product of glycerol fermentation employing many microbial species such as *Clostridium*,⁶ *Klebsiella*, *Citrobacter*,⁷ *Lactobacillus*,⁸ and of genetically modified microorganisms.⁹ The low crude glycerol price could lead to these feeds becoming the preferred substrates for microbial 1,3-PDO production. Since our report¹⁰ on the combination of *Clostridium butyricum* activity with hydrogen transfer chemocatalysis to convert crude glycerol from biodiesel production, further studies focused on direct crude glycerol fermentations have been reported.^{11,12,13} The conversion of glycerol to 1,3-PDO employs two enzymatic steps: glycerol dehydration by glycerol dehydratase to 3-hydroxypropionaldehyde, and its further reduction to 1,3-PDO by NADH dependent 1,3-propanediol oxidoreductase.⁹ This reductive metabolic pathway is used by microorganism to

maintain the steady state concentration of NADH and NAD⁺ cofactors.^{9,13} Concentrations as high as 93.7 g/l of 1,3-PDO from pure and 76.2 g/l of 1,3-PDO from crude glycerol with productivities of 3.3 and 2.3 g/l-h, respectively, have been reported¹¹ for fed-batch anaerobic production by *Clostridium butyricum* isolates. The main bottleneck of fermentative production of 1,3-PDO and its further applications for chemical catalysis is the formation of by-products such as butyrate, ethanol and acetate.⁵ These products contaminate the fermentation broth and complicate the downstream processing, and further developments are required on the isolation of the products of whole cell biocatalysis.

Following this biocatalytic step, the intermediate chemical must be extracted from the aqueous solution and converted into a marketable chemical. Extraction from water can be difficult and expensive, particularly as the chemicals generated often have high water solubility, and this has led to research into the application of newer solvent technologies. In the field of bio-renewable alcohol extraction from aqueous solution ionic liquids are showing considerable promise. Ionic liquids exhibit the dual advantages of tuneable physical properties, and high affinity for alcohols. The functional groups comprising the cation and anion can be tuned to alter solvent properties, and hydrophobic ionic liquids can be prepared.¹⁴ Hydrophobic ionic liquids still have excellent solubilising properties for polar organics; this enables the biphasic extraction of fermentation broth to be set up. The efficient extraction of bio-butanol has been demonstrated using imidazolium¹⁵ and phosphonium¹⁶ ionic liquids, and the optimisation of 1,3-propanediol extraction is ongoing in several research groups, including Marr and co-workers (X. Liu *et al* unpublished work). Varying the class of cation or anion, and even the functionality for a given ionic liquid type, changes the properties of extraction markedly. For ionic liquids that are not sufficiently hydrophobic, the addition of salts to the aqueous phase can yield biphasic mixtures to enable oxygenated targets to be selectively extracted.¹⁷⁻²⁰ Recently this approach has been applied to the removal of 1,3-propanediol from fermentation broths.^{21,22}

Once extracted into the ionic liquid, the desired organic product must be isolated. Extraction with a volatile organic solvent will render the initial extraction barely worthwhile! However, the primary product of fermentation is rarely the desired chemical target, and can be viewed as a chemical intermediate. Coupling biocatalysis with a downstream chemocatalytic reaction without intermediate isolation can avoid separation problems.^{3,10} Industrial scale fermentations to yield chemicals tend to be large. If a sufficient concentration of the product can be obtained, the aqueous solution could be drawn off and converted to chemical products or fuels as required. Ideally the extraction, downstream reaction, and

product removal will not contaminate the fermentation broth, and will render it recyclable, therefore conserving water. In a special case a functional ionic liquid could act as the extracting solvent and catalyst for chemical change,²² but instances in which the catalyst and extraction solvent optimise coincidentally will be exceptional. Alternatively the addition of a catalyst to the extracting solvent is acceptable, provided the catalyst does not leach into the aqueous solution.

New chemocatalytic transformations that can be coupled to biocatalytic 1,3-PDO production are being investigated by Marr and co-workers.^{3,10,23} Of specific interest is the potential of hydrogen transfer and dehydrogenation catalysts to transform bio-renewable alcohols into value added chemicals.^{24,25}

Reactions that involve the transfer of hydrogen from one organic donor to another (sometimes termed “hydrogen borrowing” reactions) have huge potential in organic synthesis, and have been the subject of several recent reviews.^{24–39} Typically these reactions employ a transition metal catalyst (most commonly an organometallic Ru or Ir complex) and a base to activate an alcohol by deprotonation and extraction of hydride from the α -position. The unsaturated group thus formed can then go on to participate in the formation of new C-N and C-C bonds. In this way a wide range of alcohols can act as the source of an alkyl group for alkylation, the most common substrates being amines or carbonyls. These methods avoid the use of activating leaving groups and halides, and do not lead to the formation of salt waste. In this way alkylated amines, carboxylic acids, amides and nitrogen containing heterocycles can be prepared.

The activation of 1,3-propanediol by hydrogen transfer and its use to prepare 1,3-diamino propanes by *N*-alkylation of secondary amines was demonstrated by Huh *et al.* employing $\text{RuCl}_3 \cdot n\text{H}_2\text{O}$ as the catalyst precursor in dioxane at 180 °C.⁴⁰ In boiling diglyme, quinolines result from the dehydrogenation initiated amination of 1,3-PDO in the presence of aniline catalysed by phosphine (P^nBu_3) promoted ruthenium (III) chloride.⁴¹

An alternative procedure has been published by Madsen and co-workers⁴² including the addition of $\text{MgBr}_2 \cdot \text{OEt}_2$ to the catalytic system as a promoter, and expanding the procedure to the synthesis of a range of functionalised quinoline derivatives. Treatment of naphthylamines with 1,3-PDO in the presence of $\text{IrCl}_3 \cdot n\text{H}_2\text{O}$ promoted by BINAP enables *N*-heterocyclization in an analogous manner.⁴³ Avoiding the dehydrogenation of the *N*-heterocyclized product, and therefore performing a dehydrative coupling, Achard and co-workers⁴⁴ have prepared (functionalised) julolidines from tetrahydroquinolines and 1,3-PDO. Pentamethylcyclopentadienyl iridium(III) chloride dimer $[\text{Cp}^*\text{IrCl}_2]_2$ was employed as the

catalyst precursor, promoted by diphenylphosphinobenzoic acid. The reaction was performed at 130 °C in toluene. Cp*Ir(III) complexes have wide applicability in reactions that involve the removal and transfer of hydrogen to activate alcohols; in addition to the well established transfer amination protocols,^{25,30,33} many other organic hydrogen transfer and dehydrogenation reactions are possible, for example Oppenauer-type oxidation,⁴⁵ dehydrogenation,^{29,36,46} the Guerbet reaction,⁴⁷⁻⁴⁹ and dynamic kinetic resolution.⁵⁰⁻⁵⁴

Previously Marr, Rebros and co-workers demonstrated that 1,3-PDO generated from the fermentation of crude glycerol from biodiesel can act as the substrate for the *N*-alkylation of aniline.¹⁰ A Cp*Ir(III) *N*-heterocyclic carbene hydrogen transfer catalyst was employed in ionic liquid or toluene assisted by simple carbonate salts. When amination is operated in ionic liquid solvents,^{10,55} we previously noted²³ that the substrate showed a tendency towards simultaneous dehydration. The resulting aldehydes can react together by aldol condensation and couple to yield C6 products. This cascade follows a similar mechanism to the Guerbet reaction.^{47,48} The potential importance of Guerbet chemistry in bio-renewable transformations has been underlined recently, as a method of transforming bio-ethanol to bio-butanol.⁵⁶ The application of ionic liquid solvents and alteration of the concentration of amine were later shown to enable control over the reaction selectivity.²³

Here is reported the use of a homogeneous hydrogen transfer catalyst to catalyse the dehydration of 1,3-propanediol in ionic liquid to propionaldehyde (propanal). This follows the report of amination by hydrogen transfer by coupled bio- and chemo-catalysis,^{10,23} and has the additional benefit of easier product separation. By assisting a dehydration reaction, the catalyst and ionic liquid remove oxygen from the bio-alcohol, and this reduces hydrogen bonding, rendering the organic products more volatile and easier to remove from the solvent. To the best of our knowledge, this is the first report on the selective transformation of 1,3-PDO into propionaldehyde. The production of aldehydes is targeted due to their importance in chemical synthesis,^{57,58} being precursors for carboxylic acids and esters, olefins, amines, amides and higher aldehydes and alcohols. Hundreds of thousands of tonnes of propionaldehyde are prepared worldwide per year. The leading production method is the hydroformylation of ethene derived from petroleum. Bulk uses of propionaldehyde include the synthesis of trimethylolthane (and its derivatives) for the production of resins, coatings, plasticisers and lubricants. Propionaldehyde is also used extensively in the organic synthesis of fine chemicals. The high purity aldehydes required for pharmaceuticals, foods and fragrances are particularly valuable, and have higher market values than the parent alcohols. Cp*IrCl₂(NHC) (Cp* = pentamethylcyclopentadienyl; NHC = carbene ligand) complex **1**

(See Figure 1) and base were applied to 1,3-PDO in ionic liquid; the major products observed were propionaldehyde (**2**), 2-methyl-pentenal (**3**), 2-methyl-pentanal (**4**), and 1-propanol (**5**) (See Scheme 1 (a)).

Experimental

1,3-Propanediol (98 % w, Aldrich), K₂CO₃ (99.5 % w, BDH), KOH (85 % w, Riedel-de Haen), Cs₂CO₃ (99.995 % w, Sigma-Aldrich), propionaldehyde (97 % w, Aldrich), 2-methyl-2-pentenal (97 % w, Aldrich), 2-methyl-pentanal (> 95.0 % w, TCI), propanol (97 % w, Sigma-Aldrich), CH₃OH (≥ 99.9 % w, CHROMASOLV, for HPLC, Sigma-Aldrich), CDCl₃ (99 % w, Aldrich), CD₃C(O)CD₃ (VWR Chemicals), were used as received. **1**,⁵⁹ 1-ethyl-2,3-dimethyl-imidazolium-*N,N*-bistriflimide (EmmimNTf₂),⁶⁰ and methyl-tri-*n*-octyl-ammonium-*N,N*-bistriflimide (N_{1,8,8,8}NTf₂)⁶¹ (Figure 1), were synthesized according to literature procedures. ¹H NMR spectra were run on 300 MHz and 400 MHz Bruker spectrophotometers. The chemical shifts are reported in ppm. Signal multiplicities are reported as singlet (s), doublet (d), triplet (t), quartet (qrt), and multiplet (m) (br = broad). GC/MS spectroscopic data were collected on a MassHunter Workstation Software – Qualitative Analysis – Version B.06.00 – Build 6.0.663.10 – Service Pack 1 – © Agilent Technologies, Inc. 2012. GC/MS column: Agilent Technologies, Inc.; 19091S-433UI; HP-5MS UI; 30 m X 0.250 mm; 0.25 Micron; –60 to 325/350C; SN: USE137316H. GC/MS spectroscopic data were processed on MassHunter Data Analysis – MassHunter GC/MS Acquisition B.07.01.1805 – 12-Mar-2014 – © 1989-2014 Agilent Technologies.

Hydrogen transfer initiated dehydration (HTID) of 1,3-propanediol (1,3-PDO) in the presence of **1** and a base, in ionic liquid: screening reaction conditions.

1,3-PDO, **1**, a base, and an ionic liquid (see Table S8) were added to a 50 mL round bottom flask connected, through a distillation condenser, to a 50 mL glass tube. The mixture was reacted at the selected temperature, at a controlled pressure of *ca.* 0.35 bar, for six hours, stirring at 1000 rpm. The reaction product, a colourless liquid, was isolated by distillation, being collected, for the duration of the six hours reaction, in the collecting glass tube kept at *ca.* -196 °C (N₂ (l) bath). After separation from the minor water layer, the crude product (see % yield (based on propionaldehyde (**2**) in Table S8) was analysed by GC/MS (Table S18) and ¹H NMR (Table S27) spectroscopies. The reacted mixture, left in the 50 mL round bottom flask, was analysed by ¹H NMR spectroscopy. The crude product was distilled at

atmospheric pressure, at $T \cong 43$ °C, to yield **2**. ^1H NMR (CDCl_3 , 400 MHz): δ_{H} 1.09 (td, $J_{\text{HH}} = 7.42$, $J_{\text{HH}} = 1.10$ Hz, 3 H), 2.45 (m, 2 H), 9.78 (m, 1 H).

Detailed procedures for the recycling experiments are given in the supplementary data file.

Analysis of reaction product solutions of HTID of 1,3-PDO in the presence of 1 and a base, in ionic liquids: general methodology.

The amount of **5** in the isolated crude product was calculated *via* GC/MS spectroscopy. Integration of the ^1H NMR spectrum allowed calculation of the molar amounts of **2**, **3** and **4**, relative to **5**. Combination of GC/MS and ^1H NMR spectroscopic information enabled calculation of the amount of **2**, **3** and **4**, in the isolated crude product.

The GC/MS and ^1H NMR analysis of reaction product solutions are described in the supplementary data file.

Results and discussion

Treatment of 1,3-PDO in ionic liquid solution with a base and a $\text{Cp}^*\text{IrCl}_2(\text{NHC})$ complex has been found to lead to dehydration to yield aldehydes.²³ The hydrogen transfer initiated dehydration (HTID) of 1,3-PDO was investigated in the presence of complex **1** and a base, in an ionic liquid as the solvent medium. The outcome of the reaction was explored in different ionic liquids, at different temperatures and pressures, and by varying the catalyst loading and the nature and loading of the base. Product solutions were analysed by a combination of ^1H NMR and GC/MS spectroscopies.

The ionic liquids reported (Figure 1) could be used to extract 1,3-propanediol from fermentation broth, as they are hydrophobic due to the presence of the NTf_2 anion, but they do not represent an optimized system for fermentation broth extraction. EmmimNTf_2 and $\text{N}_{1,8,8,8}\text{NTf}_2$ are examples of two very common classes of ionic liquid. An in depth study and optimization of the extraction is ongoing as part of the EU FP7 project GRAIL and many ionic liquids are being screened. At the same time the fermentation of glycerol to 1,3-PDO is being optimized and this is leading to an increase in the concentration of 1,3-propanediol that is achievable in solution, which has a direct effect on the ability to extract it efficiently.

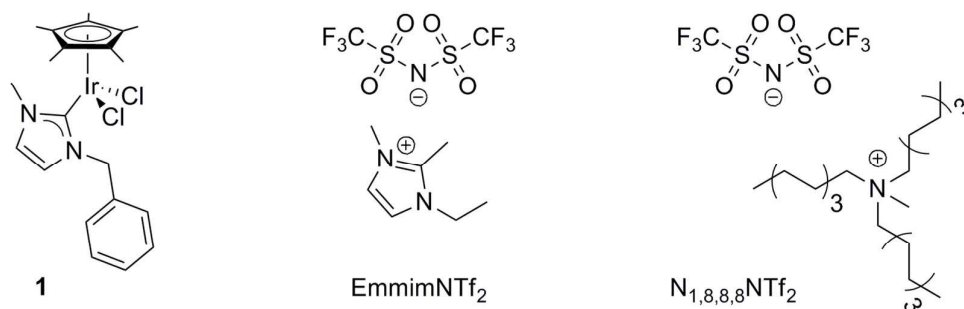
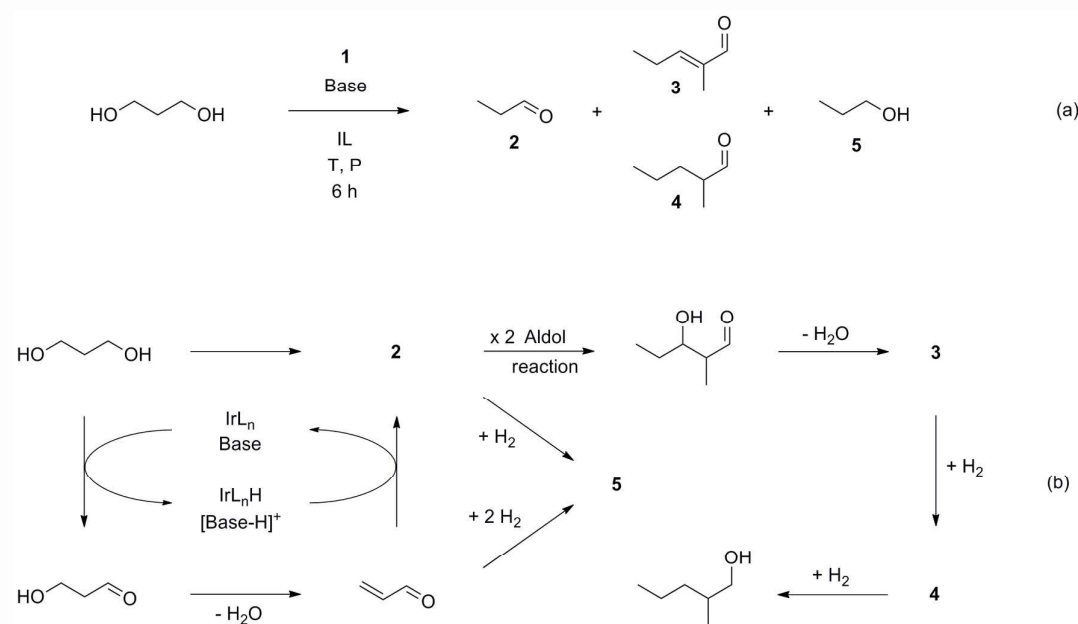


Figure 1. Structure of catalyst **1** and 1-ethyl-2,3-dimethyl-imidazolium-*N,N*-bistriflimide (EmmimNTf₂) and methyl-tri-*n*-octyl-ammonium-*N,N*-bistriflimide (N_{1,8,8,8}NTf₂), ionic liquids tested as the solvent media, in the Cp*IrX₂(NHC) catalysed HTID of 1,3-PDO.

The reaction was found to lead to a range of C3 and C6 alcohols and aldehydes: the major products observed were **2**, **3**, **4**, and **5** (Scheme 1 (a)). The reaction outcome was found to be affected by the experimental conditions: reaction yield and selectivity could be controlled by tuning (a) the ionic liquid used as the solvent, the reaction (b) temperature and (c) pressure, (d) the loading of **1**, and (e) the nature and loading of the base. The synthesis and isolation of **2** was first targeted.



Scheme 1. HTID of 1,3-PDO catalysed by Cp*IrX₂(NHC) complex **1** in the presence of a base, in ionic liquids, at different temperatures and pressures: (a) major reaction products; (b) postulated reaction mechanism.

A postulated reaction sequence for the HTID of 1,3-PDO catalysed by Cp*IrX₂(NHC) complexes in the presence of a base, that rationalises the formation of the major products, is shown in Scheme 1 (b). HTID of 1,3-PDO allows formation of **2** via the intermediates 3-

hydroxypropionaldehyde and acrolein. The formation of the dimer of acrolein was observed previously under similar conditions.²³ Both **2** and acrolein could then undergo hydrogenation to **5**. Furthermore, **2** can dimerise *via* the aldol reaction to yield, after dehydration, **3**. **3** can then undergo further hydrogenation to **4**. Hydrogenation of the latter leads to 2-methylpentanol. In addition to the main reaction sequence, the intermediate 3-hydroxypropionaldehyde could undergo a retro-aldol reaction to yield formaldehyde and acetaldehyde. Formaldehyde is a possible source of hydrogen, through dehydrogenation. Hydrogen can also be formed by dehydrogenation of alkyl chains to form olefins. The formation of traces of acetaldehyde and olefins are consistent with spectra obtained.

According to Scheme 1 (b) the formation of C6 products depends upon the aldol reaction of **2** in solution. The selectivity of the reaction should depend on the concentration of **2**. Therefore the reaction outcome should be driven towards specific target compounds by tuning the reaction conditions. Running the HTID of 1,3-PDO in ionic liquids under conditions that allow the removal of **2** from the reaction mixture as soon as it is formed should minimise, the occurrence of the side-reactions leading to **3**, **4** and **5**. Conversely, higher selectivity towards these products should be favoured when allowing **2** to further react after its formation.

The HTID of 1,3-PDO was therefore successfully driven towards the selective production of **2** by reacting 1,3-PDO in the presence of the Ir(III) complex **1** ([1,3-PDO]:[Ir] = 73.2 – 496.7; (see Table 1, Table 2, and tables S1 – S7) and a base (K₂CO₃, or KOH, or Cs₂CO₃; [Base]:[1,3-PDO] = 0.0302 – 0.2764), in ionic liquids EmmimNTf₂, or N_{1,8,8,8}NTf₂, at temperature varying in the range 100 – 180 °C, and at a dynamic vacuum of *ca.* 0.35 bar. The vacuum allowed removal of the highly volatile **2** out of the reaction mixture as soon as it was formed; then, a low temperature trap allowed isolation of the crude product (see Figure S16) in high yield (up to 99 %), and highly rich in **2**. 1,3-PDO was found to be completely consumed after six hours; the reaction outcome was then investigated after six hours. Selectivity towards **2** varied, depending on the reaction conditions, in the range 25.5 – 87.5 %. The rest 74.5 – 12.5 % of product was found to be composed by **3**, **4** and **5**, along with minor amounts of other side-products. Selectivity towards **3**, **4** and **5** varied in the range 2.8 - 61.2 %, 0.0 - 17.5 %, 3.3 - 56.7 %, respectively.

The ¹H NMR spectra of the isolated, crude product of HTID of 1,3-PDO at the above conditions (see Figure 2) display, in the aldehydic region, the triplet at δ_H 9.78 due to the aldehydic proton of the largely dominant species, **2**, along with the doublet at δ_H 9.60 and the singlet at δ_H 9.38 corresponding to the aldehydic protons of **4** and **3**, respectively; the triplet

detected at δ_{H} 3.59 is due to the CH_2OH protons of **5**. Consistently, the GC/MS spectrum of the corresponding solutions (see Figure S1) displays the peaks due to **2**, **3**, **4** and **5**.

EmmimNTf₂ and N_{1,8,8,8}NTf₂ are stable throughout the six hours reaction time: no decomposition of the ionic liquids was observed under any experimental conditions tested. The reacting mixtures were monitored by ¹H NMR spectroscopy: the resonances due to the protons of EmmimNTf₂ and N_{1,8,8,8}NTf₂ remain unchanged throughout the reaction time (see Figure S4 and Figure S8, respectively).

The catalytic system is not sensitive to air, and the reaction is not affected by the presence of significant amounts of water (Table S7).

Mercury poisoning experiments showed the Cp*Ir systems to be homogeneous: **1** displayed virtually unperturbed activity in the presence of mercury, strongly suggesting genuine solution-phase catalysis (Table 2).⁶²

The involvement of a monohydride iridium complex^{62,63} derivative of the catalytic precursor **1**, as intermediate in the catalytic cycle ruling the base-assisted HTID of 1,3-PDO, is suggested by the ¹H NMR investigation of the reacting mixture: after running the HTID of 1,3-PDO, in the presence of **1** and K₂CO₃, in N_{1,8,8,8}NTf₂, at 150 °C, for three hours, a sole singlet at δ_{H} -16.54 was observed in the hydride region (see Figure S14). In EmmimNTf₂, along with the largely major singlet at δ_{H} -16.57, a minor peak at δ_{H} -16.09 is also observed (see Figure S15). The ¹H NMR resonance of the hydride (in CDCl₃) lies in the expected range for terminal hydride complexes, by comparison with similar complexes reported previously.⁶⁴⁻⁶⁷ Further mechanistic work is required to comment on the role of such monohydride iridium complex in the catalytic cycle.

Complex **1** was monitored by ¹H NMR whilst running the HTID of 1,3-PDO in the presence of **1** and K₂CO₃, in N_{1,8,8,8}NTf₂, (analysis in EmmimNTf₂ was hampered by solvent-signal overlap), at T 150 °C, and at [1,3-PDO]:[Ir] \cong 220.0. The doublet at δ_{H} 6.02 (J_{HH} = 15.3 Hz), due the methylenic protons of **1**, was monitored during the course of the reaction. The catalyst precursor **1** was observed in the reaction mixture for *ca.* two hours since the reaction started. Several overlapping resonances were detected in the region δ_{H} 5.00 – 7.00 since the beginning of the reaction, preventing any further speculation regarding the nature of the active Ir complex formed in solution. The doublet at δ_{H} 6.02 was observed collapsing *ca.* three hours after starting the reaction. Further investigation will be carried out in order to understand the nature of the active catalytic Ir species.

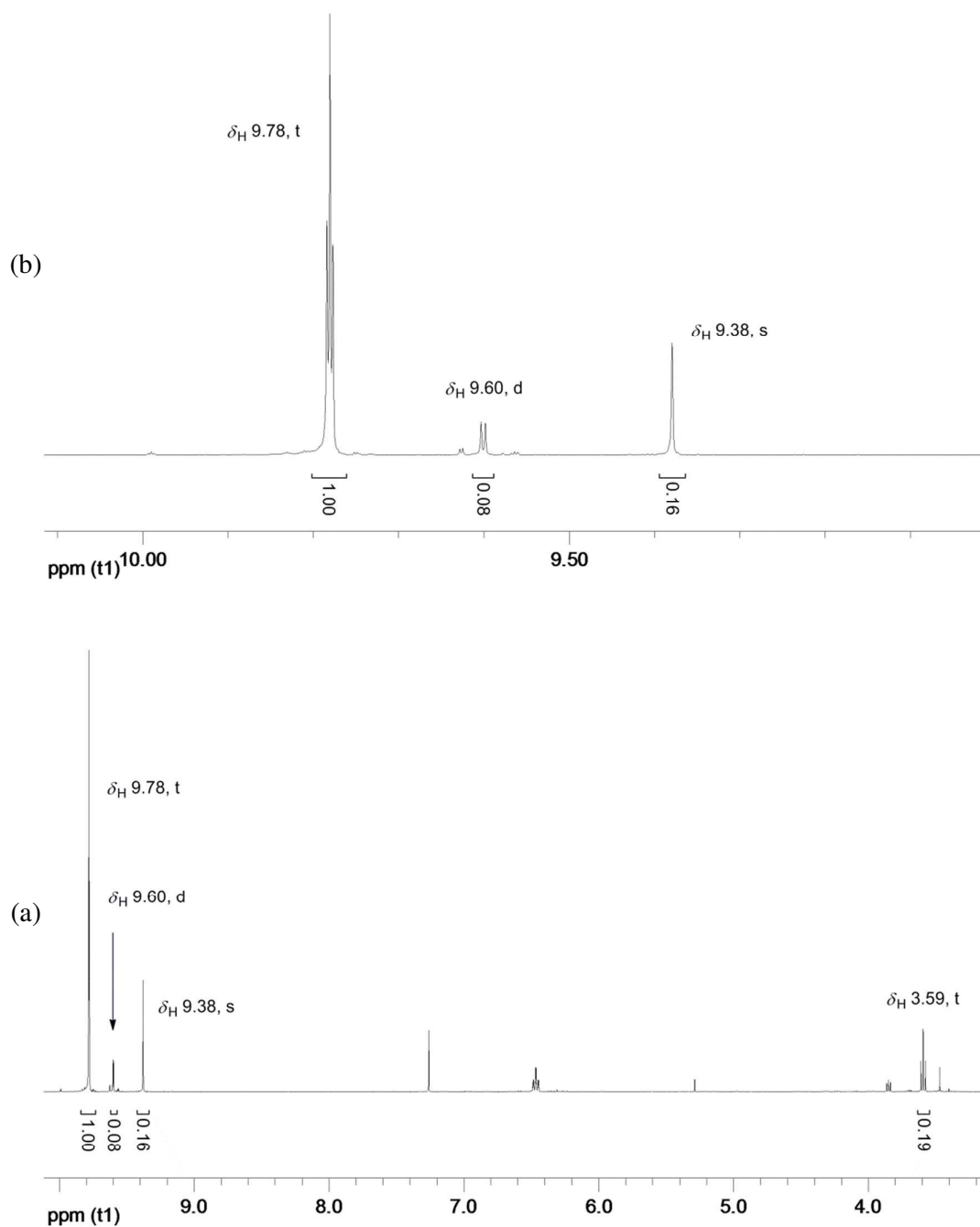


Figure 2. Example of a ¹H NMR spectrum of the isolated, crude product of HTID of 1,3-PDO in the presence of **1** and a base, in EmmimNTf₂ or N_{1,8,8,8}NTf₂, at temperature varying in the range 100 – 180 °C, and at a dynamic vacuum of *ca.* 0.35 bar: enlargement of the aldehydic and 1-propanol CH₂OH region (δ_{H} 3.10 - δ_{H} 10.10) (a); enlargement of the aldehydic region (δ_{H} 9.00 - δ_{H} 10.12) (b).

The non-volatility of the ionic liquid, along with the much lower boiling point of **2** (46.0 °C) compared to that of the by-products (**3**: 137.5 °C; **4**: 119.5 °C; **5**: 97.0 °C) allowed then the facile separation of **2**. The isolation of highly pure **2** was achieved *via* a mild distillation

at P_{atm} and $T = 43\text{ }^{\circ}\text{C}$. The ^1H NMR spectrum of the distilled, isolated product (Figure S2) only displays resonances due to **2**: a triplet at δ_{H} 9.78, a quartet of doublets at δ_{H} 2.45, and a triplet at δ_{H} 1.10. Consistently, only the peaks due to **2** are displayed in the GCMS spectrum of the distilled, isolated product (Figure S3). In conclusion, highly pure **2** was produced *via* HTID of 1,3-PDO, catalysed by **1** in the presence of a base, in ionic liquids, followed by a mild distillation. To the best of our knowledge, this is the first report on the selective transformation of 1,3-PDO into **2**. **2** was only reported as a very minor component in the product mixture of dehydrogenation of 1,3-PDO, performed in several, extreme conditions.⁶⁸⁻⁷⁰

The influence of (a) the ionic liquid used as the solvent, (b) the catalyst loading, the reaction (c) temperature and (d) pressure, and (e) the nature and loading of the base on the selectivity towards the C3 and C6 aldehydes and alcohols and the yields of **2** was then investigated (see Table 1).

The catalyst **1** and the base are indispensable: in the absence of the iridium catalyst, 1,3-PDO remains unreacted; also, no reaction of 1,3-PDO is observed when the HTID is carried out in the presence of **1** but in the absence of base (In Table 1: see entries 17 and 18, respectively).

The ionic liquids tested as the solvent media were EmmimNTf₂ and N_{1,8,8,8}NTf₂. The imidazolium cation is C2 protected with a methyl group to prevent side reactions involving deprotonation and the formation of carbenes. The ammonium ionic liquid was chosen as a cheaper alternative to the more common imidazolium ionic liquids. The bis(trifluoromethylsulfonyl)imide (NTf₂) anion confers hydrophobicity, ensuring the solvent forms two phases with water, and enabling a biphasic extraction of fermentation broth.

Yields and selectivities towards **2** are generally higher in EmmimNTf₂ than N_{1,8,8,8}NTf₂ (Table 1: entries 3 and 23; 7 and 26; 9 and 25; 16 and 30). Although ionic liquids have been selected as solvents for the reaction primarily in order to enable a facile separation of the final, volatile products from the non-volatile solvent media (and also, prior to chemocatalysis, in the prospect of allowing extraction of 1,3-PDO from the aqueous glycerol fermentation broths), it was found that their use also affects the reaction outcome: while little effect on yields was observed, selectivity towards **2** was found to significantly improve in ionic liquids when compared to HTID of 1,3-PDO carried out in the absence of ionic liquid (Table 1: entries 7, 19, and 26). We have previously shown that ionic liquids support greater dehydration activity than toluene under related conditions.^{10,23}

It is also worthy of note that when the HTID of 1,3-PDO was carried out in neat 1,3-PDO, in molar concentrations corresponding to those of $N_{1,8,8,8}NTf_2$ (Table 1: entry 31) and $EmmimNTf_2$ solvents (Table 1: entry 32), the catalyst was found to turnover at a greater frequency. In these reactions the selectivity towards **2** was lower than for the optimised ionic liquid system.

The effect of catalyst loading on the yield of and selectivity towards **2** was investigated varying the ratio [1,3-PDO]:[Ir] in the range *ca.* 70.0 - *ca.* 500.0. While no significant effect on selectivity was observed, catalyst loading affects the yields of **2**: the lower the ratio [1,3-PDO]:[Ir], the higher the yield (Table 1: entries 5, 6, 7, and 8; 20 and 25; 21 and 26; 22, and 27). In both $EmmimNTf_2$ and $N_{1,8,8,8}NTf_2$, only traces amount of **2** were observed to be formed when [1,3-PDO]:[Ir] > *ca.* 220.0.

Only a minor effect on the reaction outcome was observed when changing the base: yields and product distributions were similar when using either K_2CO_3 , KOH or Cs_2CO_3 (Table 1: entries 7, 12, and 16; 26, 28, and 30). K_2CO_3 was then selected as the base for the HTID of 1,3-PDO catalysed by **1**. Yields of and selectivity towards **2** were affected by the base molar concentration: the higher the base concentration the lower the yield of, and selectivity towards **2** (Table 1: entries 7, 14, and 15). This may suggest that the higher base concentration stimulates side-reactions, which could include dehydrogenation, retro-aldol, and orthometallation⁵⁹ of **1**. The HTID of 1,3-PDO was found to perform best when $[K_2CO_3]:[1,3-PDO] \cong 0.0310$.

The effect of the reaction temperature has been explored in the range 80 – 180 °C. Satisfying yields of and selectivity towards **2** were achieved at temperatures $120 \leq T \leq 150$ °C, in both $EmmimNTf_2$ and $N_{1,8,8,8}NTf_2$, and at a ratio [1,3-PDO]:[Ir] varying in the range *ca.* 70.0 - *ca.* 220.0. Minor conversions are observed at $T < 100$ °C (Table 1: entries 4 and 24). In the range 100 – 150 °C, the higher the temperature, the higher the yields of and selectivity towards **2**, at any ratio [1,3-PDO]:[Ir] and in both $EmmimNTf_2$ and $N_{1,8,8,8}NTf_2$ (Table 1: entries 1, 2, 3, and 4; 21, 22, 23, and 24). Raising the temperature to 180 °C resulted in little improvement, and similar amounts of isolated **2** were formed (entries 7 and 9; 20 and 21): the ¹H NMR spectra of the isolated crude products show formation of further by-products containing alkenic protons, suggesting an increase in dehydrogenation activity. It is worth noting that selectivity towards **2** fails under 100 °C: selectivity towards **3** was found to increase up to 61.2 % when running the HTID of 1,3-PDO in $N_{1,8,8,8}NTf_2$ at 80 °C, while selectivity towards **2** was 25.5 % (Table 1: entry 4).

Table 1. HTID of 1,3-PDO in the presence of **1** and a base, in ionic liquids: yields^a of **2**, selectivity towards **2**, **3**, **4**, and **5**, and TOF.

Entry	Solvent	Catalyst	[1,3-PDO]:[Ir]	Base	[Base]:[1,3-PDO]	T	% Yield ^a (2)	2	3	4	5	TOF ^b [s ⁻¹] (×10 ³)
1	N _{1,8,8} NTf ₂	1	74.8	K ₂ CO ₃	0.0310	150	84	85.9	5.9	1.5	6.7	2.90
2	N _{1,8,8} NTf ₂	1	73.2	K ₂ CO ₃	0.0311	120	60	52.9	28.3	9.8	9.0	2.02
3	N _{1,8,8} NTf ₂	1	76.1	K ₂ CO ₃	0.0302	100	27	70.4	12.1	13.1	4.4	0.96
4	N _{1,8,8} NTf ₂	1	75.6	K ₂ CO ₃	0.0313	80	1	25.5	61.2	0.0	13.2	0.04
5	N _{1,8,8} NTf ₂	1	73.3	K ₂ CO ₃	0.0308	150	84	75.2	10.4	5.1	9.3	2.83
6	N _{1,8,8} NTf ₂	1	98.9	K ₂ CO ₃	0.0309	150	69	72.2	14.9	7.3	5.6	3.16
7	N _{1,8,8} NTf ₂	1	219.9	K ₂ CO ₃	0.0303	150	51	76.2	11.8	6.4	5.5	5.23
8	N _{1,8,8} NTf ₂	1	496.7	K ₂ CO ₃	0.0310	150	6	78.2	10.8	6.6	4.4	1.44
9	N _{1,8,8} NTf ₂	1	217.0	K ₂ CO ₃	0.0316	180	49	82.0	7.1	4.2	6.8	4.96
10	N _{1,8,8} NTf ₂	1	73.6	KOH	0.0545	150	78	78.4	9.5	4.0	8.1	2.65
11	N _{1,8,8} NTf ₂	1	74.8	KOH	0.0536	100	11	73.0	8.8	9.9	8.3	0.39
12	N _{1,8,8} NTf ₂	1	218.7	KOH	0.0541	150	62	84.2	2.8	2.8	5.7	6.26
13	N _{1,8,8} NTf ₂	1	218.3	KOH	0.0496	100	2	39.3	4.1	0.0	56.7	0.18
14	N _{1,8,8} NTf ₂	1	219.8	K ₂ CO ₃	0.1365	150	29	52.1	24.3	11.5	12.1	2.99
15	N _{1,8,8} NTf ₂	1	218.1	K ₂ CO ₃	0.2764	150	20	54.1	22.4	12.8	10.6	2.07
16	N _{1,8,8} NTf ₂	1	207.3	CsCO ₃	0.0321	150	17	78.1	10.8	2.6	8.5	1.58
17	N _{1,8,8} NTf ₂	No catalyst	/	K ₂ CO ₃	0.0312	150	/	/	/	/	/	/
18	N _{1,8,8} NTf ₂	1	220.9	No base	/	150	/	/	/	/	/	/
19	No IL	1	226.6	K ₂ CO ₃	0.0311	150	69	55.6	27.8	12.2	4.3	7.20
20	EmmimNTf ₂	1	75.2	K ₂ CO ₃	0.0309	180	85	72.5	12.5	3.7	11.3	2.97
21	EmmimNTf ₂	1	75.1	K ₂ CO ₃	0.0315	150	78	73.0	10.1	8.6	8.3	2.72
22	EmmimNTf ₂	1	75.6	K ₂ CO ₃	0.0307	120	74	73.3	13.9	7.4	5.3	2.60
23	EmmimNTf ₂	1	74.7	K ₂ CO ₃	0.0311	100	60	69.2	7.2	17.5	6.1	2.09
24	EmmimNTf ₂	1	74.8	K ₂ CO ₃	0.0312	80	1	67.3	3.5	25.0	4.2	0.04
25	EmmimNTf ₂	1	221.9	K ₂ CO ₃	0.0314	180	62	77.1	10.6	3.9	8.4	6.35
26	EmmimNTf ₂	1	219.7	K ₂ CO ₃	0.0315	150	70	72.7	12.5	6.1	8.6	7.07
27	EmmimNTf ₂	1	225.8	K ₂ CO ₃	0.0304	120	51	80.3 ^c	8.0 ^c	9.6 ^c	2.0 ^c	5.33
28	EmmimNTf ₂	1	226.1	KOH	0.0555	150	54	85.2	5.9	1.4	7.5	5.68
29	EmmimNTf ₂	1	74.5	KOH	0.0540	80	1	37.3	5.8	41.5	15.4	0.04
30	EmmimNTf ₂	1	220.2	CsCO ₃	0.0313	150	67	82.9	5.7	2.8	8.6	6.85
31	1,3-PDO	1	350.9	K ₂ CO ₃	0.0068	150	- ^d	61.2	24.3	10.3	4.1	10.28 ^d
32	1,3-PDO	1	203.2	K ₂ CO ₃	0.0118	150	- ^d	66.3	18.3	9.0	6.5	7.03 ^d

All operations were carried out (a) at P = 0.35 bar; (b) with reaction time: 6 h; (c) at RPM: 1000. ^a Crude, isolated product. ^b TOF = n(product formed) / [n(catalyst) × time]. ^c Calculations based on ¹H NMR (See Table S18, entry 27). ^d In entries 31 and 32, 1,3-PDO was used as both the substrate and the solvent.

The recyclability of the catalytic system generated by precursor **1** towards the HTID of 1,3-PDO was investigated in both EmmimNTf₂ and N_{1,8,8,8}NTf₂. In the presence of K₂CO₃, at 120 and 150 °C and 0.35 bar, at catalyst loading [1,3-PDO]:[Ir] \cong 75.0 and 220.0, **1** was found to be a highly recyclable catalyst precursor. The base was found to be unstable and further aliquots of base were required to attain good recycling. Reloading only with **1**, in the absence of additional base, the catalyst activity collapsed almost entirely after the first cycle when testing the recyclability in N_{1,8,8,8}NTf₂, at 150 °C and 0.35 bar, at catalyst loading [1,3-PDO]:[Ir] \cong 75.0. In EmmimNTf₂, under the same conditions, still reloading only with **1**, the crude product yield fell from 78 % to 54 % and then 29 % from the first to the second and then third cycle, respectively, showing significant, quick decrease in catalyst activity.

In EmmimNTf₂, the catalyst was found to be recyclable for at least 10 catalytic runs at 150 °C and at catalyst loading [1,3-PDO]:[Ir] \cong 75.0. No significant loss of activity or selectivity towards **2** was observed (Figure 3, and Table S1): the percentage yield of crude **2** varied in the range 75 – 99 % (1st catalytic run: 82 %; 10th catalytic run: 75 %) (Figure 3 (a)); the selectivity towards **2** varied in the range 65.3 – 71.7 % (Figure 3 (b)).

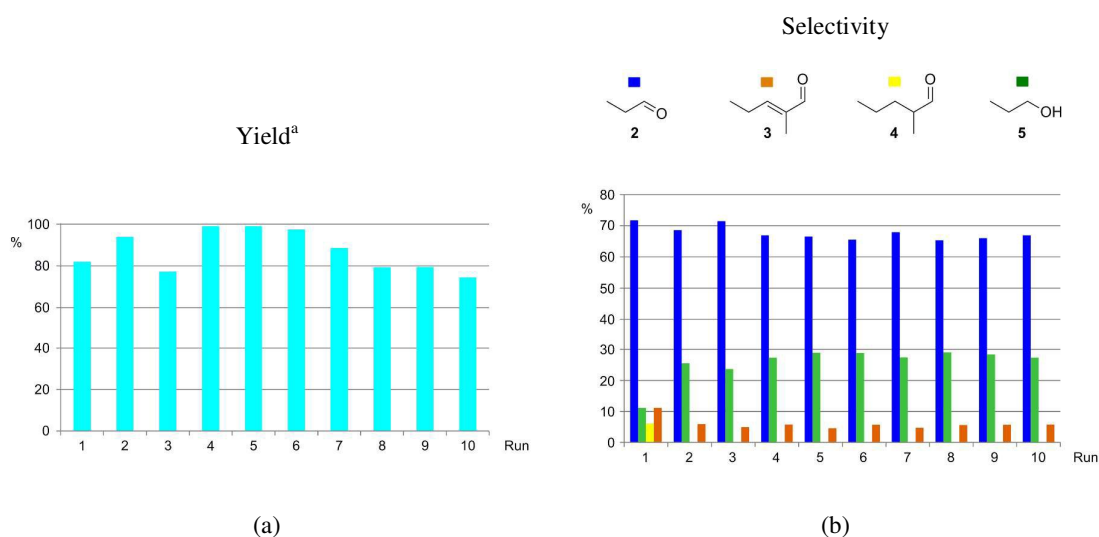


Figure 3. Recycling **1** as catalyst precursor towards HTID of 1,3-PDO ([1,3-PDO]:[Ir] \cong 75.0) in EmmimNTf₂, in the presence of K₂CO₃, at 150 °C and 0.35 bar: (a) yield of crude **2**; (b) selectivity towards **2**, **3**, **4**, and **5**. ^a Crude, isolated product.

The recyclability of **1**, proven to be effective over the 10 catalytic runs at 150 °C and [1,3-PDO]:[Ir] \cong 75.0, was then tested, and successfully confirmed, at different temperatures and catalyst loadings, over 5 catalytic runs. At 150 °C and [1,3-PDO]:[Ir] \cong 220.0 (Table S2), very little changes in the percentage yields of crude **2** were observed over the 5 catalytic runs

(1st catalytic run: 73 %; 5th catalytic run: 74 %) (Figure 4 (a)). Also, the reaction remained highly selective towards **2** (% of **2**: 1st catalytic run, 77.6 %; 5th catalytic run, 76.2 %) (Figure 4 (b)). When testing the recyclability of **1** at 120 °C and [1,3-PDO]:[Ir] \cong 75.0 over 5 catalytic runs (Table S3), the percentage yields of crude **2** varied in the range 72 - 79 % (1st catalytic run: 72 %; 5th catalytic run: 78 %) (Figure 5 (a)), while the selectivity towards **2** varied in the range 71.2 – 76.2 % (Figure 5 (b)).

The ionic liquid EmmimNTf₂ is stable throughout the 10 and 5 recycling runs, at any of the above experimental conditions: the ¹H NMR spectrum of the CDCl₃ solutions of the reacting mixture after the six hours reaction shows that the triplet at δ_{H} 1.51 and the singlets at 2.64, and 3.83, due to the methylic protons, the quartet at δ_{H} 4.14, due to the methylenic protons, and the singlet at δ_{H} 7.19, due to the alkenic protons of EmmimNTf₂, remain unchanged throughout the reaction time of each of the 10 and 5 recycling runs (see Figure S4).

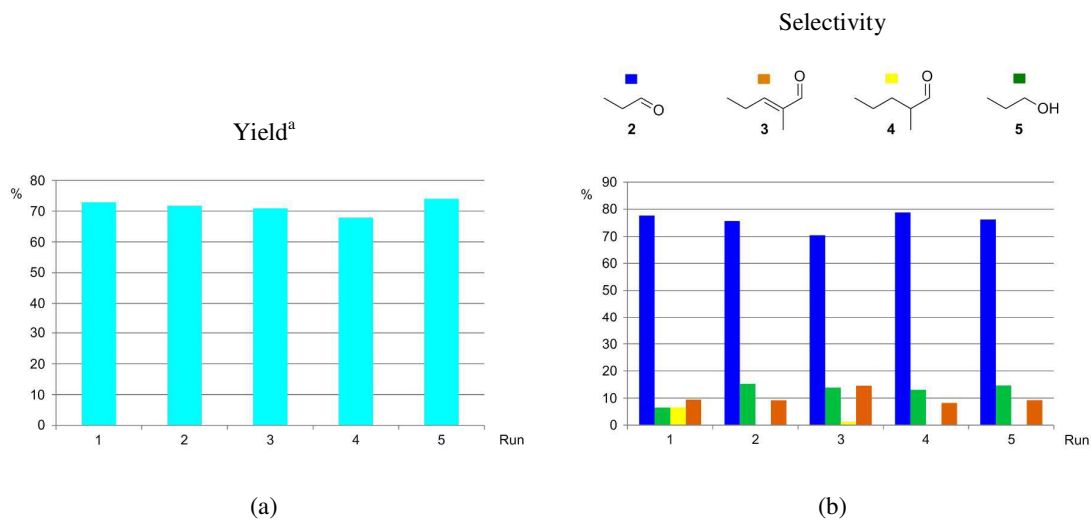


Figure 4. Recycling **1** as catalyst precursor towards HTID of 1,3-PDO ([1,3-PDO]:[Ir] \cong 220.0) in EmmimNTf₂, in the presence of K₂CO₃, at 150 °C and 0.35 bar: (a) yield of crude **2**; (b) selectivity towards **2**, **3**, **4**, and **5**. ^a Crude, isolated product.

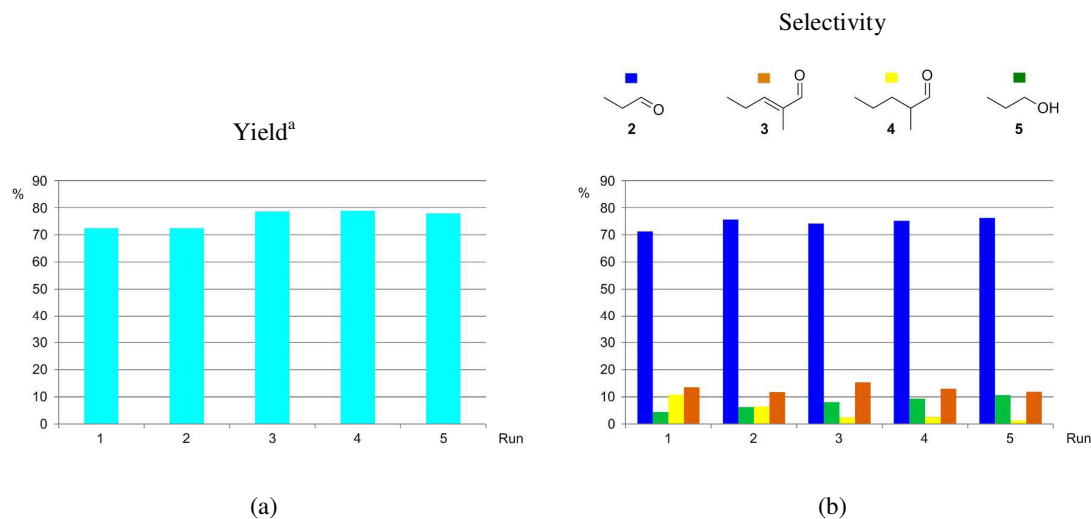


Figure 5. Recycling **1** as catalyst precursor towards HTID of 1,3-PDO ([1,3-PDO]:[Ir] \cong 75.0) in EmmimNTf₂, in the presence of K₂CO₃, at 120 °C and 0.35 bar: (a) yield of crude **2**; (b) selectivity towards **2**, **3**, **4**, and **5**. ^a Crude, isolated product.

1 is recyclable also in $N_{1,8,8,8}NTf_2$. High selectivity towards **2** was observed over the 10 catalytic runs when testing the catalyst recycling at 150 °C and $[1,3-PDO]:[Ir] \cong 75.0$ (% of **2**: 1st catalytic run, 83.9 %; 10th catalytic run, 73.4 %) (Table S6 and Figure S7 (b)), and over the 5 catalytic runs at 150 °C and $[1,3-PDO]:[Ir] \cong 220.0$ (% of **2**: 1st catalytic run, 87.5 %; 5th catalytic run, 82.2 %) (Table S4 and Figure S5 (b)) and at 120 °C and $[1,3-PDO]:[Ir] \cong 75.0$ (% of **2**: 1st catalytic run, 81.3 %; 5th catalytic run, 76.0 %) (Table S5 and Figure S6 (b)).

At 150 °C and $[1,3-PDO]:[Ir] \cong 220.0$, the percentage yield of crude **2** was found to be 60 % in the 1st run and 57 % in the 5th run, with maximum and minimum values of 62 % (3rd run) and 48 % (2nd run), respectively (Figure S5 (a)). At 120 °C and $[1,3-PDO]:[Ir] \cong 75.0$, the percentage yield of crude **2** varied in the range 44 - 67 %, and was found almost identical in the 1st (59 %) and 5th run (60 %) (Figure S6 (a)). More fluctuation in the percentage yields of crude **2** was observed over the 10 catalytic runs when testing the recyclability of **1** at 150 °C and at $[1,3-PDO]:[Ir] \cong 75.0$ in $N_{1,8,8,8}NTf_2$ (Figure S7 (a)), when compared to $EmmimNTf_2$. The percentage yield of crude **2**, after dropping from 86 % (1st run) to 22 % (2nd run), was found to vary in the range 54 - 77 % from the 3rd to the 10th catalytic run (3rd catalytic run: 54 %; 10th catalytic run: 58 %).

The ionic liquid $N_{1,8,8,8}NTf_2$ is also stable throughout the 10 and 5 recycling runs, at any of the above experimental conditions: the ¹H NMR spectra of the $CDCl_3$ solutions of the reacting mixture after the six hours reaction show that the triplet at δ_H 0.88 due to the $-CH_2CH_3$ methylic protons, the broad multiplets at δ_H 1.31 and 1.64 due to the $-CCH_2C-$ methylenic protons, the singlet at 3.01 due to the $-NCH_3$ methylic protons, and the multiplet at δ_H 3.18 due to the $-NCH_2-$ methylenic protons of $N_{1,8,8,8}NTf_2$, remain unchanged during the course of the reaction for each of the 10 and 5 recycling runs (Figure S8).

Table 2. Mercury poisoning test of the iridium precatalyst in HTID of 1,3-PDO in the presence of **1** and K₂CO₃, in EmmimNTf₂, at T 150 °C: yields^a of **2**, selectivity towards **2**, **3**, **4**, and **5**, and TOF.

[1,3-PDO]:[Ir]	[Base]:[1,3-PDO]	% Yield ^a (2)	2	3	4	5	TOF ^b [s ⁻¹] (×10 ³)
206.3	0.0312	77	78.0	9.4	6.6	6.0	7.32

The reaction was carried out (a) at P = 0.35 bar; (b) with reaction time: 6 h; (c) at RPM: 1000. ^aCrude, isolated product. ^b TOF = n(product formed) / [n(catalyst) × time].

Further investigation of the HTID of 1,3-PDO will be aimed at targeting other value-added chemicals. The reaction parameters will be tuned in order to drive the reaction outcome selectively towards the other products. Allowing propionaldehyde to further react after its formation should increase the percentage of C6 aldehydes, compared to propionaldehyde, in the reaction mixture. Amongst them, 2-methyl-pentenal is a valuable chemical.⁵⁸

Conclusions.

We have shown that complex **1** forms a highly recyclable catalyst for the selective production of a range of C3 and C6 aldehydes *via* homogeneous HTID of 1,3-PDO in ionic liquids. The successful isolation of highly pure propionaldehyde can be easily achieved under reduced pressure, and distillation, with minimal waste. In addition HTID of 1,3-PDO in ionic liquids is successful also when significant volumes of water are involved in the reaction, and in the presence of air. The successful synthesis and isolation of value-added chemicals out of the ionic liquid solutions of 1,3-PDO (mimicking the product of extraction of aqueous glycerol fermentation broth) proves that the combination of Cp*IrX₂(NHC) catalysed HTID of 1,3-PDO in ionic liquids with bio-catalysis has, ultimately, the potential to allow the transformation of waste glycerol into valuable chemicals that can be simply isolated. This valorisation of waste to chemicals would add significant value and improve the economics of biomass waste utilization.

Acknowledgements

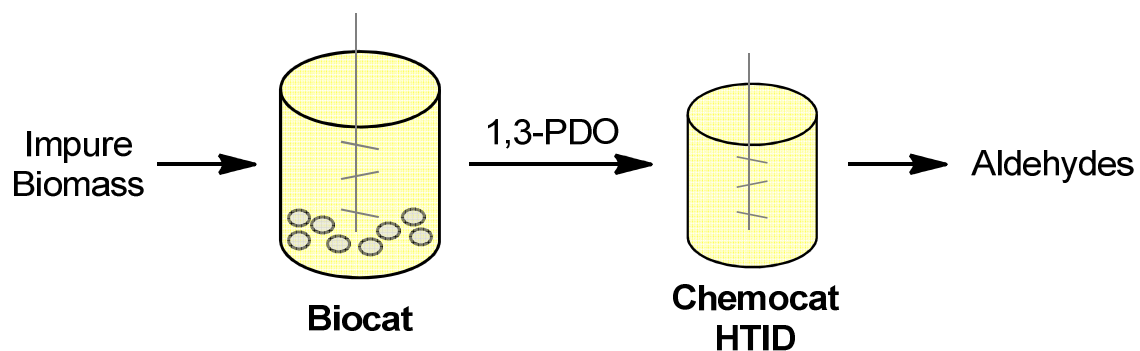
This work was supported by GRAIL (Grant agreement no: 613667), project co-financed by the European Commission under the 7th Framework Programme. The assistance provided by Queen's University Ionic Liquid Laboratories (QUILL), and the analytical chemistry service (ASEP) and glassblowing service at Queen's University Belfast, is acknowledged.

Notes and references

1. U.S. Department of Energy (2004) Top Value Added Chemicals from Biomass (Vol. 1) (Ed's T. Werpy and G. Petersen), Pacific Northwest National Laboratory (PNNL), National Renewable Energy Laboratory (NREL), Office of Biomass Program (EERE). <http://www.eere.energy.gov/>.
2. T. Banner, A. Fosmer, H. Jessen, E. Marasco, B. Rush, J. Veldhouse and M. De Souza, "Biocatalysis for Green Chemistry and Chemical Process Development," ed's J. Tao and R. Kazlauskas, Wiley, New Jersey, 2011, 429–467.
3. A. C. Marr and S. F. Liu, *Trends Biotech.*, 2011, **29**, 199–204.
4. US6013494, Jan 11 2000, C. E. Nakamura, A. A. Gatenby, A. Kuang-Hua Hsu, R. D. La Reau, S. L. Haynie, M. Diaz-Torres, D. E. Trimbur, G. M. Whited, V. Nagarajan, M. S. Payne, S. K. Picataggio, R. V. Nair,

- “Method for the production of 1,3-propanediol by recombinant microorganisms”, A, E. I. Du Pont De Nemours And Company, Genencor International.
5. C.S. Lee, M.K. Aroua, W.M.A.W. Daud, P. Cognet, Y. Pérès-Lucchese, P-L Fabre, O. Reynes, and L. Latapie, *Renew. Sust. Energ. Rev.* 2015, **42**, 963–972.
 6. P. Kubiak, K. Leja, K. Myszka, E. Celinska, M. Spychała, D. Szymanowska-Powałowska, K. Czaczyk, and W. Grajek, *Process Biochem.*, 2012, **47**, 1308–1319.
 7. R.K. Saxena, P. Anand, S. Saran, and J. Isar, *Biotechnol. Adv.*, 2009, **27**, 895–913.
 8. M. A. Ricci, A. Russo, I. Pisano, L. Palmieri, M. de Angelis, and G. Agrimi, *J. Microbiol. Biotechnol.* 2015, **25**, 893–902.
 9. C. E. Nakamura and G. M. Whited, *Curr. Opin. Biotech.* 2003, **14**, 454–459.
 10. S. F. Liu, M. Rebros, G. Stephens and A. C. Marr, *Chem. Commun.*, 2009, 2308–2310.
 11. E. Wilkens, A. K. Ringel, D. Hortig, T. Willke, and K.-D. Vorlop, *Appl. Microbiol. Biotechnol.*, 2012, **93**, 1057–1063.
 12. D. Dietz and A.-P. Zeng, *Bioprocess Biosyst. Eng.*, 2014, **37**, 225–233.
 13. R. Dobson, V. Gray, K. Rumbold, *J. Ind. Microbiol. Biotechnol.*, 2012, **39**, 217–226.
 14. P. Bonhôte, A-P Dias, M. Armand, N. Papageorgiou, K. Kalyanasundaram and M. Grätzel, *Inorg. Chem.*, 1996, **35**, 1168–1178.
 15. M. Stoffers and A. Górak, *Sep. Purif. Technol.* 2013, **120**, 415–422.
 16. D. Rabari and T. Banerjee, *Ind. Eng. Chem. Res.*, 2014, **53**, 18935–18942.
 17. K. E. Gutowski, G. A. Broker, H. D. Willauer, J.G. Huddleston, R. P. Swatloski, J. D. Holbrey, and R. D. Rogers, *J. Am. Chem. Soc.*, 2003, **125**, 6632–6633.
 18. J.-Y. Dai, Y.-Q. Sun, and Z.-L. Xiu, *Eng. Life Sci.* 2014, **14**, 108–117.
 19. M.G. Freire, A. F. Cláudio, J. M. Araújo, J. A. Coutinho, I. M. Marrucho, J. N. Canongia Lopes, and L. P. Rebelo, *Chem. Soc. Rev.* 2012, **41**, 4966–4995.
 20. A. Müller, and A. Górak, *Sep. Purif. Technol.* 2012, **97**, 130–136.
 21. A. Müller, R. Schulz, J. Wittmann, I. Kaplanow, and A. Górak, *RSC Advances*, 2013, **3**, 148–156.
 22. M. Matsumoto, K. Nagai, and K. Kondo, *Solvent Extr. Res. Dev.*, 2015, **22**, 209–213.
 23. S. D. Lacroix, A. Pennycook, S. Liu, T. T. Eisenhart and A. C. Marr, *Catal. Sci. Technol.*, 2012, **2**, 288–290.
 24. A. C. Marr, *Catal. Sci. Technol.*, 2012, **2**, 279–287.
 25. M. Pera-Titus, and F. Shi, *ChemSusChem*, 2014, **7**, 720–722.
 26. M. Haniti, S. A. Hamid, P. A. Slatford, and J. M. J. Williams, *Adv. Synth. Catal.* 2007, **349**, 1555–1575.
 27. G. Guillena, D. J. Ramón, and M. Yus, *Angew. Chem. Int. Ed.* 2007, **46**, 2358–2364.
 28. T. D. Nixon, M. K. Whittlesey, and J. M. J. Williams, *Dalton Trans.*, 2009, 753–762.
 29. G. E. Dobereiner, and R. H. Crabtree, *Chem. Rev.* 2010, **110**, 681–703.
 30. G. Guillena, D. J. Ramón, and M. Yus, *Chem. Rev.* 2010, **110**, 1611–1641.
 31. A. J. A. Watson and J. M. J. Williams, 2010, *Science*, 2010, **329**, 635–636.
 32. O. Saidi, and J. M. J. Williams, *Top. Organomet. Chem.* 2011, **34**, 77–106.
 33. S. Bähn, S. Imm, L. Neubert, M. Zhang, H. Neumann, and M. Beller, *ChemCatChem*, 2011, **3**, 1853–1864.
 34. Y. Obora, and Y. Ishii, *Synlett*, 2011, 30–51.
 35. S. Pan, and T. Shibata, *ACS Catal.*, 2013, **3**, 704–712.
 36. C. Gunanathan and D. Milstein, *Science*, 2013, **341**, 1229712.
 37. J. Schranck, A. Tlili, and M. Beller, *Angew. Chem. Int. Ed.* 2013, **52**, 7642 – 7644.
 38. Y. Obora, *ACS Catal.*, 2014, **4**, 3972–3981.
 39. M. Pera-Titus and F. Shi, *ChemSusChem*, 2014, **7**, 720–722.
 40. K.-T. Huh, S. C. Shim, and C. H. Doh, *Bull. Korean Chem. Soc.*, 1990, **11**, 45–49.
 41. Y. Tsuji, K.-T. Huh, and Y. Watanabe, *J. Org. Chem.*, 1987, **52**, 1673–1680.
 42. R. N. Monrad, and R. Madsen, *Org. Biomol. Chem.*, 2011, **9**, 610–615.
 43. H. Aramoto, Y. Obora, and Y. Ishii, *J. Org. Chem.*, 2009, **74**, 628–633.
 44. A. Labed, F. Jiang, I. Labed, A. Lator, M. Peters, M. Achard, A. Kabouche, Z. Kabouche, G. V. M. Sharma, and C. Bruneau, *ChemCatChem*, 2015, **7**, 1090–1096.
 45. F. Hanasaka, K. Fujita and R. Yamaguchi, *Organometallics*, 2004, **23**, 1490–1492.
 46. J. Wu, D. Talwar, S. Johnston, M. Yan, and J-L. Xiao, *Angew. Chem. Int. Ed.* 2013, **52**, 6983 –6987.
 47. M. Guerbet, *C. R. Acad. Sci.*, 1899, **128**, 1002–1004.
 48. M. Guerbet, *C. R. Acad. Sci.*, 1909, **149**, 129–132.

49. T. Matsu-ura, S. Sakaguchi, Y. Obora, and Y. Ishii, *J. Org. Chem.* 2006, **71**, 8306–8308.
50. A. C. Marr, C. L. Pollock and G. C. Saunders, *Organometallics*, 2007, **26**, 3283–3285.
51. R. Corberán and E. Peris, *Organometallics*, 2008, **27**, 1954–1958.
52. T. Jerphagnon, R. Haak, F. Berthiol, A. J. A. Gayet, V. Ritleng, A. Holuigue, N. Pannetier, M. Pfeffer, A. Voelklin, L. Lefort, G. Verzijl, C. Tarabiono, D. B. Janssen, A. J. Minnaard, B. L. Feringa, and J. G. de Vries, *Top. Catal.*, 2010, **53**, 1002–1008.
53. C. L. Pollock, K. J. Fox, S. D. Lacroix, J. McDonagh, P. C. Marr, A. M. Nethercott, A. Pennycook, S. Qian, L. Robinson, G. C. Saunders, and A. C. Marr, *Dalton Trans.*, 2012, **41**, 13423–13428.
54. J. G. de Vries, *Top. Catal.* 2014, **57**, 1306–1317.
55. O. Saidi, A. J. Blacker, G. W. Lamb, S. P. Marsden, J. E. Taylor, and J. M. J. Williams, *Org. Process Res. Dev.*, 2010, **14**, 1046–1049.
56. G. R. M. Dowson, M. F. Haddow, J. Lee, R. L. Wingad, and D. F. Wass, *Angew. Chem. Int. Ed.* 2013, **52**, 9005–9008.
57. R. Franke, D. Selent, and A. Börner, *Chem. Rev.* 2012, **112**, 5675–5732.
58. J. G. Stevens, R. A. Bourne, and M. Poliakoff, *Green Chem.*, 2009, **11**, 409–416.
59. R. Corberán, M. Sanaú, and E. Peris, *J. Am. Chem. Soc.* 2006, **128**, 3974–3979.
60. J. Wei, T. Ma, X. Ma, W. Guan, Q. Liu, and J. Yang, *RSC Adv.*, 2014, **4**, 30725–30732.
61. J. M. Fraile, J. I. García, C I. Herrerías, J. A. Mayoral, D. Carrié, and M Vaultier, *Tetrahedron: Asymmetry*, 2001, **12**, 1891–1894.
62. U. Hintermair, J. Campos, T. P. Brewster, L. M. Pratt, N. D. Schley, and R. H. Crabtree, *ACS Catal.*, 2014, **4**, 99–108.
63. J. S. M. Samec, J.-E. Bäckvall, P. G. Andersson, and P. Brandt, *Chem. Soc. Rev.*, 2006, **35**, 237–248.
64. T. M. Gilbert, and R. G. Bergman, *J. Am. Chem. Soc.*, 1985, **107**, 3502–3507.
65. D. S. Glueck, L. J. N. Winslow, and R. G. Bergman, *Organometallics*, 1991, **10**, 1462–1479.
66. V. Pons, and D. M. Heinekey, *J. Am. Chem. Soc.*, 2003, **125**, 8428–8429.
67. J. Campos, J. López-Serrano, E. Álvarez, and E. Carmona, *J. Am. Chem. Soc.*, 2012, **134**, 7165–7175.
68. S. Sato, R. Takahashi, T. Sodesawa, and N. Honda, *J. Mol. Cat. A: Chem.*, 2004, **221**, 177–183.
69. V. Lehr, M. Sarlea, L. Ott, and H. Vogel, *Catalysis Today*, 2007, **121**, 121–129.
70. L.-Z. Tao, S.-H. Chai, H.-P. Wang, B. Yan, Y. Liang, and B.-Q. Xu, *Catalysis Today*, 2014, **234**, 237–244.



The Hydrogen Transfer Initiated Dehydration of 1,3-propanediol to propionaldehyde was demonstrated in an ionic liquid. The reaction was catalysed by a soluble Ir(III) complex, which was highly recyclable, and air and water stable. The aldehyde was isolated under reduced pressure.

Combining Bio- and Chemo-Catalysis for the Conversion of Bio-Renewable Alcohols: Homogeneous Iridium Catalysed Hydrogen Transfer Initiated Dehydration of 1,3-Propanediol to Aldehydes

Yue-Ming Wang, Fabio Lorenzini, Martin Rebros, Graham C. Saunders,
and Andrew C. Marr.

Supplementary material

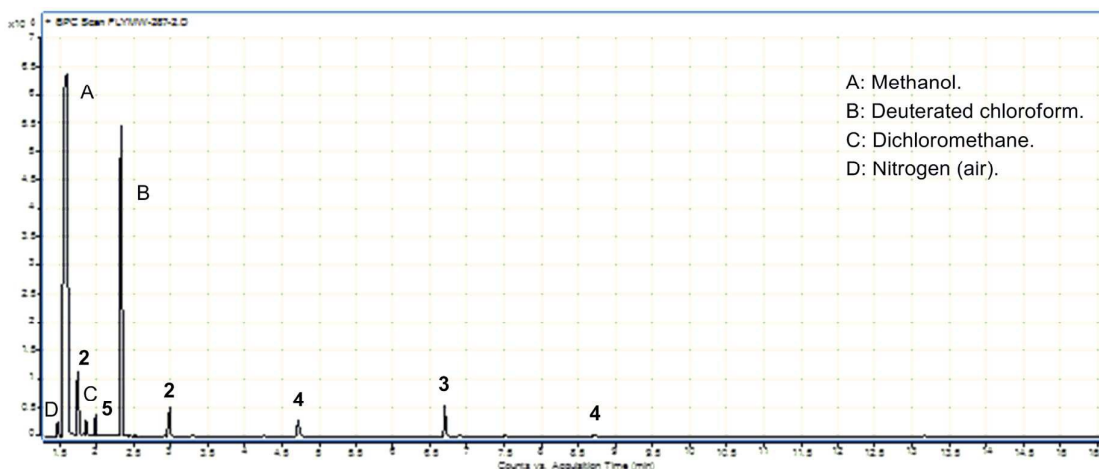


Figure S1. Example of a GC/MS spectrum of the isolated, crude product of HTID of 1,3-PDO in the presence of **1** and a base, in EmmimNTf_2 or $\text{N}_{1,8,8,8}\text{NTf}_2$, at temperature varying in the range 100 – 180 °C, and at a dynamic vacuum of *ca.* 0.35 bar. (**2**, **3**, and **4** generate, in the presence of CH_3OH , at the GC/MS experimental conditions, their hemiacetalic forms - the hemiacetalic form of **3** is not displayed in this particular GC/MS spectrum.)

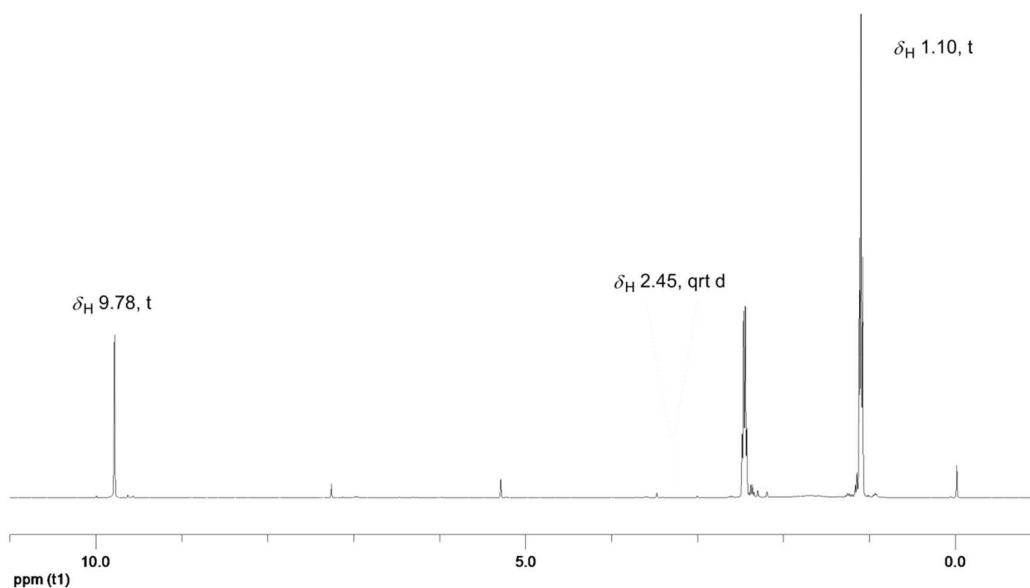


Figure S2. ¹H NMR spectrum of isolated, distilled **2**, synthesised *via* HTID of 1,3-PDO in the presence of **1** and a base, in EmmimNTf_2 or $\text{N}_{1,8,8,8}\text{NTf}_2$, at temperature varying in the range 100 – 180 °C, and at a dynamic vacuum of *ca.* 0.35 bar.

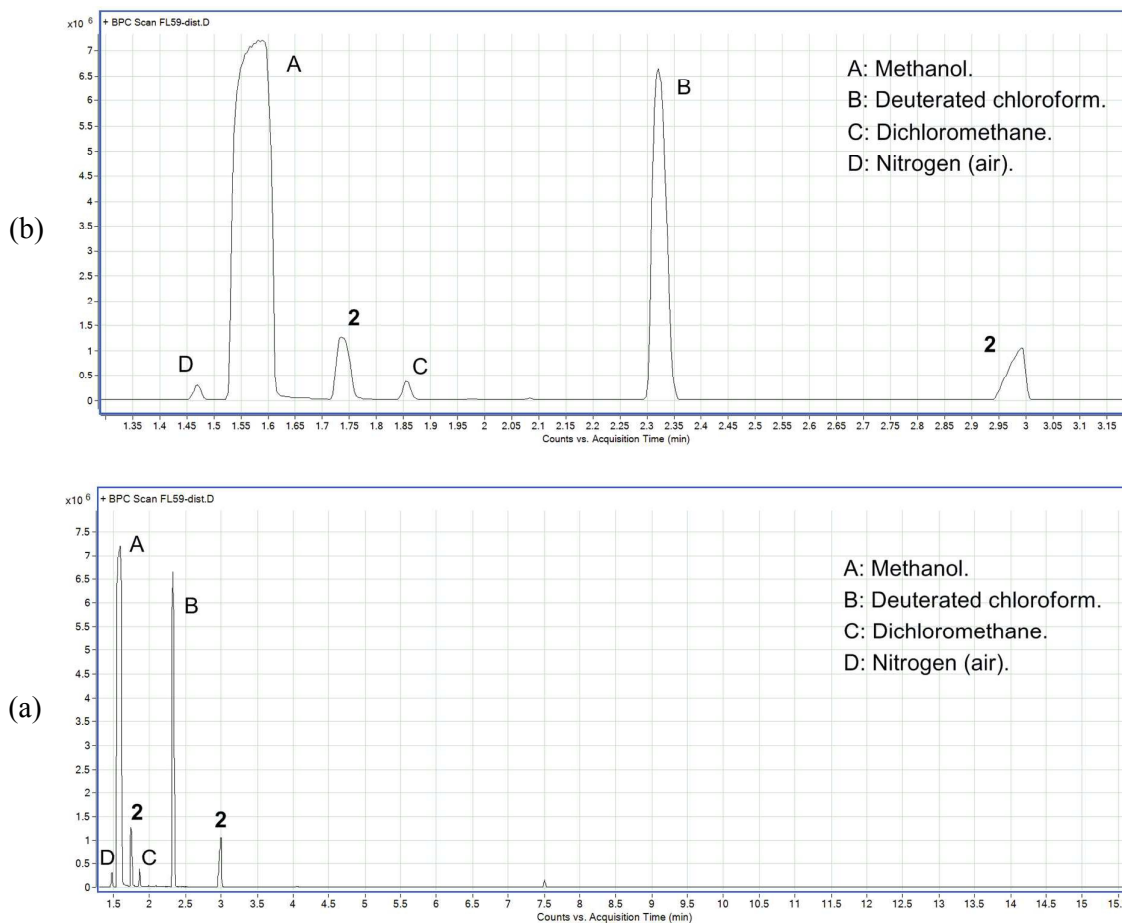


Figure S3. GCMS spectrum of isolated, distilled **2**, synthesised *via* HTID of 1,3-PDO in the presence of **1** and a base, in EmmimNTf₂ or N_{1,8,8,8}NTf₂, at temperature varying in the range 100 – 180 °C, and at a dynamic vacuum of *ca.* 0.35 bar: (a) full spectrum; (b) enlargement of the region 1.30 - 3.20 min. (**2** generates, in the presence of CH₃OH, at the GC/MS experimental conditions, its hemiacetalic form.)

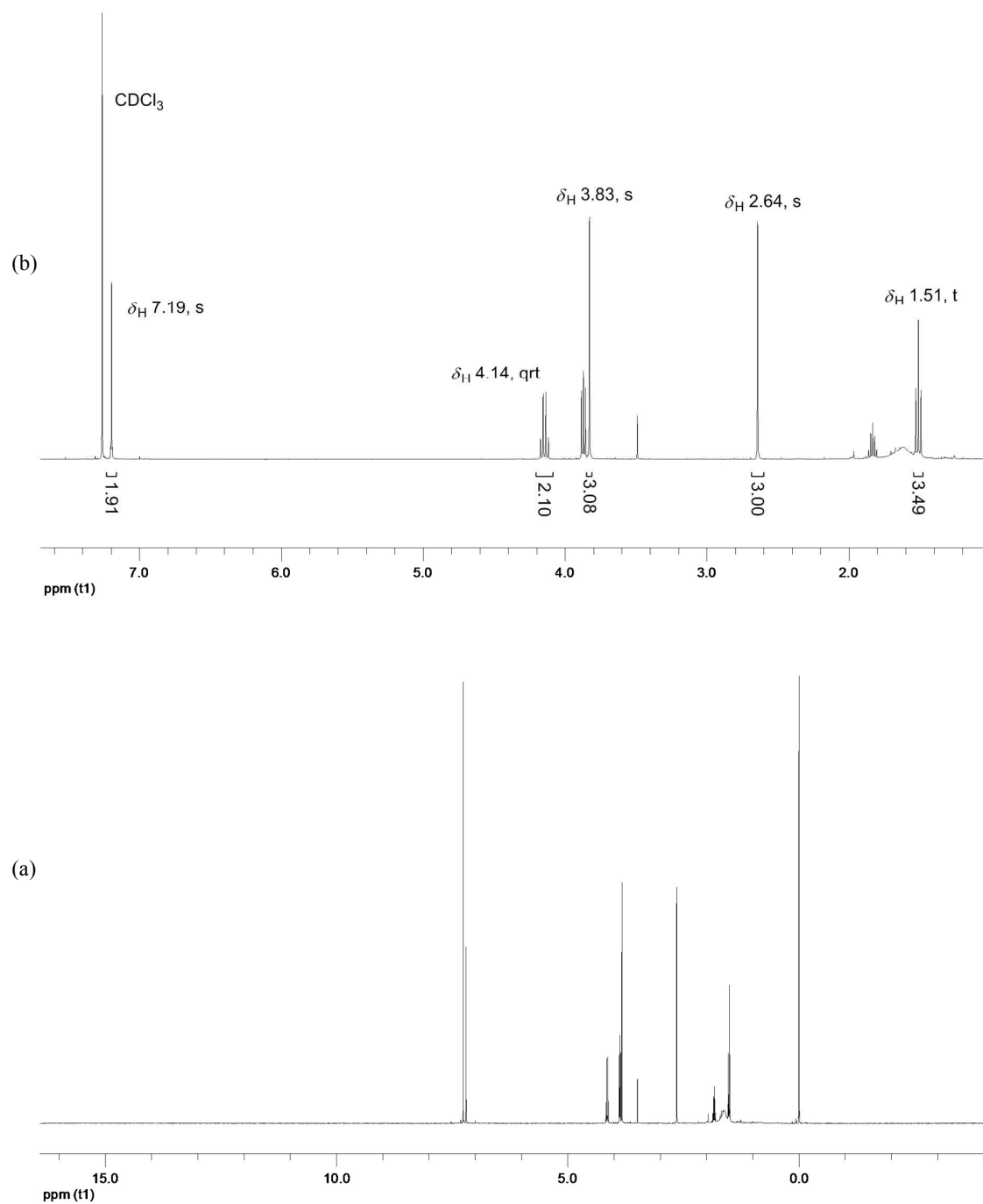


Figure S4. Recycling **1** as catalyst precursor towards HTID of 1,3-PDO in EmmimNTf₂: example of a ¹H NMR spectrum of the CDCl₃ solutions of the reacting mixture after the six hours reaction for any of the recycling runs (a: full spectrum; b: enlargement of the region δ_H 1.00 – 7.70 displaying the unchanged peaks due to EmmimNTf₂).

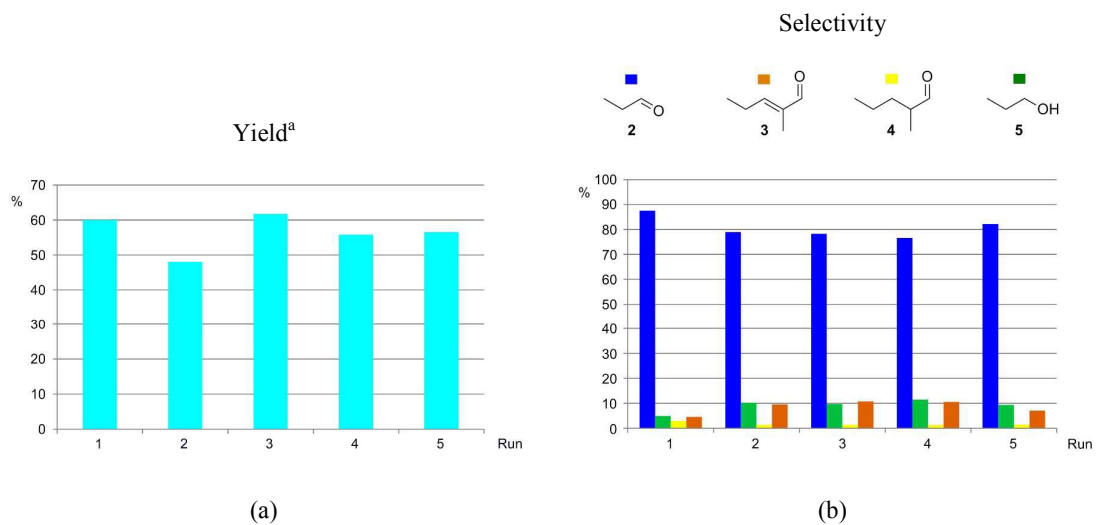


Figure S5. Recycling **1** as catalyst precursor towards HTID of 1,3-PDO ([1,3-PDO]:[Ir] \cong 220.0) in $N_{1,8,8,8}NTf_2$, in the presence of K_2CO_3 , at 150 °C and 0.35 bar: (a) yield of crude **2**; (b) selectivity towards **2**, **3**, **4**, and **5**. ^a Crude, isolated product.

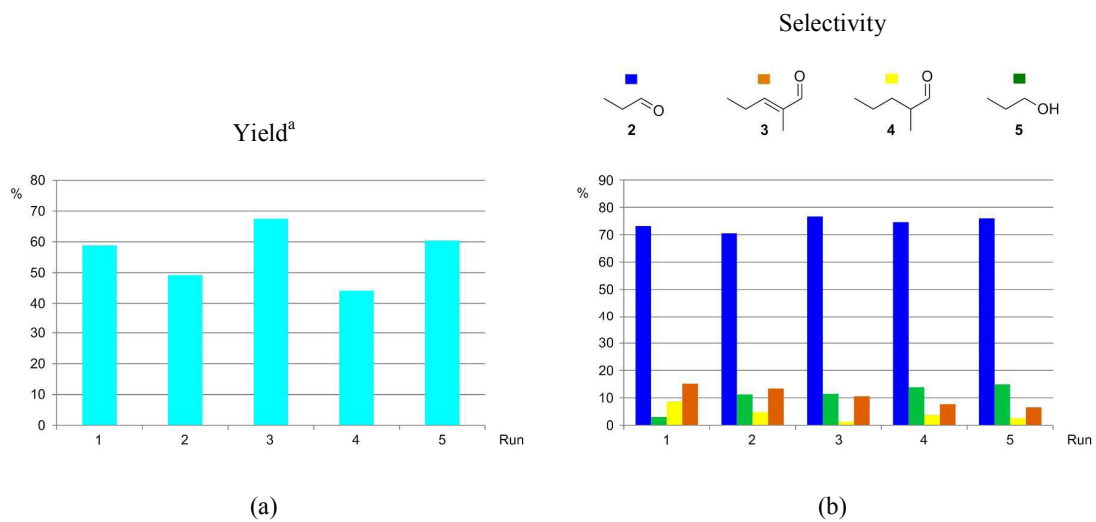


Figure S6. Recycling **1** as catalyst precursor towards HTID of 1,3-PDO ([1,3-PDO]:[Ir] \cong 75.0) in $N_{1,8,8,8}NTf_2$, in the presence of K_2CO_3 , at 120 °C and 0.35 bar: (a) yield of crude **2**; (b) selectivity towards **2**, **3**, **4**, and **5**. ^a Crude, isolated product.

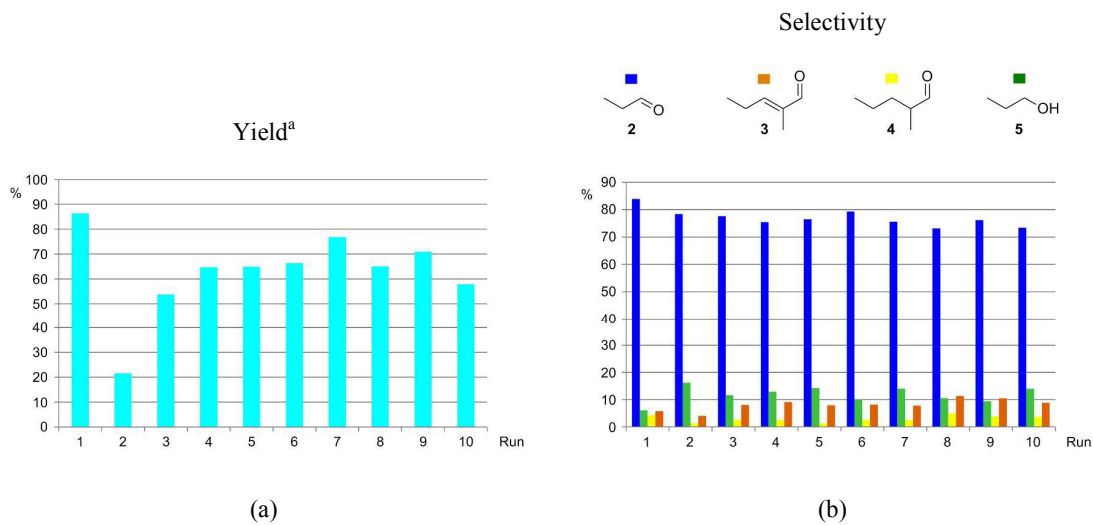


Figure S7. Recycling **1** as catalyst precursor towards HTID of 1,3-PDO ($[1,3\text{-PDO}]:[\text{Ir}] \cong 75.0$) in $\text{N}_{1,8,8,8}\text{NTf}_2$, in the presence of K_2CO_3 , at 150 °C and 0.35 bar: (a) yield of crude **2**; (b) selectivity towards **2**, **3**, **4**, and **5**. ^a Crude, isolated product.

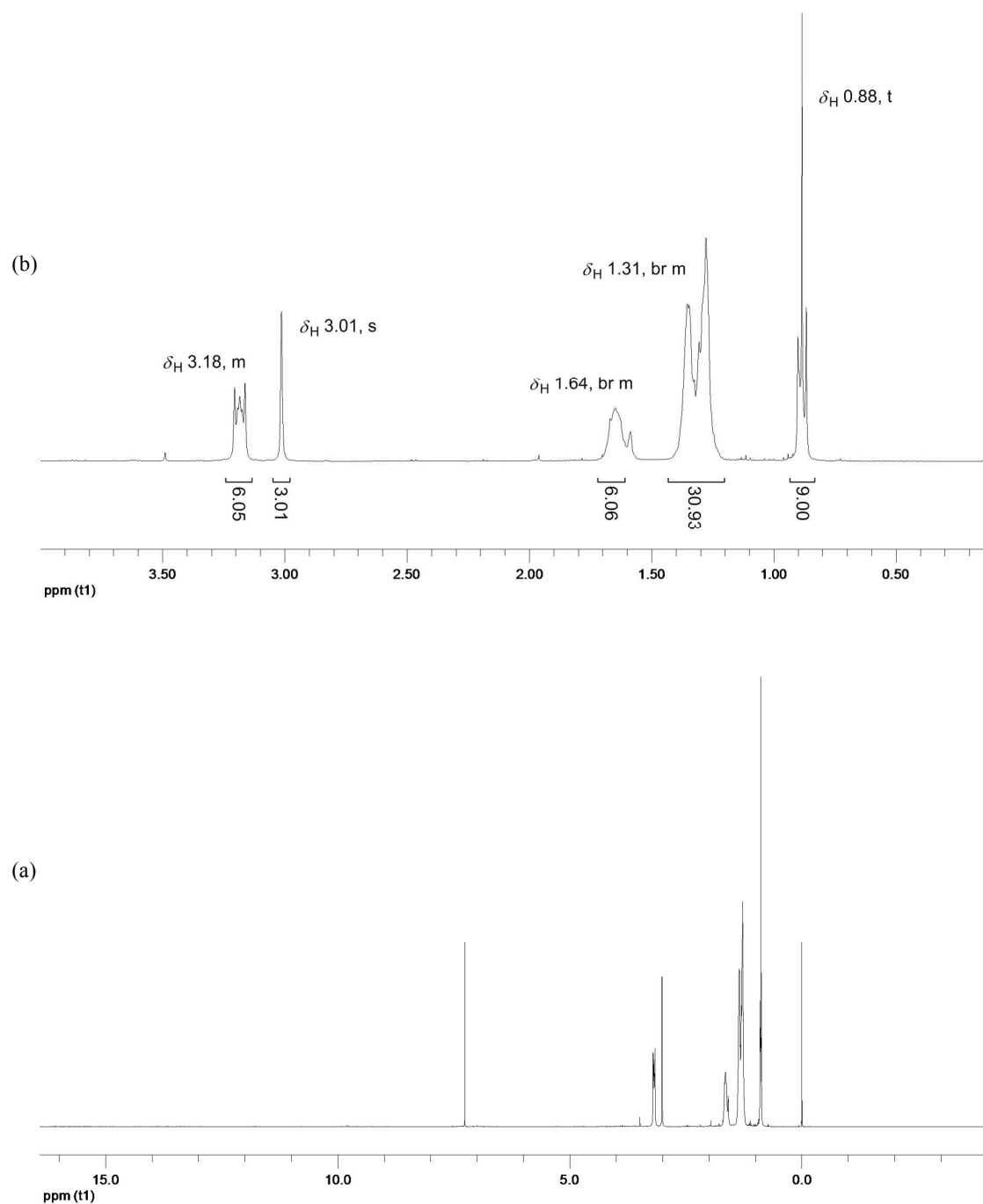


Figure S8. Recycling **1** as catalyst precursor towards HTID of 1,3-PDO in $N_{1,8,8,8}NTf_2$: example of a 1H NMR spectrum of the $CDCl_3$ solutions of the reacting mixture after the six hours reaction for any of the recycling runs (a: full spectrum; b: enlargement of the region δ_H 0.10 – 4.00 displaying the unchanged peaks due to $N_{1,8,8,8}NTf_2$).

Table S1. Recycling **1** as catalyst precursor for HTID of 1,3-PDO in the presence of K_2CO_3 , in EmmimNTf₂, at T 150 °C, and at [1,3-PDO]:[Ir] \cong 75.0: yields^a of **2**, selectivity towards **2**, **3**, **4**, and **5**, and TOF.

Entry	[1,3-PDO]:[Ir]	[Base]:[1,3-PDO]	% Yield ^a (2)	2	3	4	5	TOF ^b [s ⁻¹] ($\times 10^3$)
1	77.5	0.0303	82	71.7	11.1	6.1	11.1	2.94
2	76.5	0.0311	94	68.6	5.9	0.0	25.5	3.33
3	76.9	0.0310	77	71.4	4.9	0.0	23.7	2.75
4	76.4	0.0306	99	66.9	5.8	0.0	27.3	3.77
5	76.7	0.0304	99	66.5	4.6	0.0	28.9	3.55
6	76.4	0.0307	97	65.5	5.7	0.0	28.8	3.45
7	76.9	0.0306	89	67.9	4.7	0.0	27.4	3.15
8	75.9	0.0306	79	65.3	5.6	0.0	29.1	2.79
9	76.1	0.0308	80	66.0	5.7	0.0	28.3	2.80
10	77.0	0.0309	75	66.9	5.8	0.0	27.3	2.66

All operations were carried out (a) at P = 0.35 bar; (b) with reaction time: 6 h; (c) at RPM: 1000. ^aCrude, isolated product. ^b TOF = n(product formed) / [n(catalyst) \times time].

Table S2. Recycling **1** as catalyst precursor for HTID of 1,3-PDO in the presence of K_2CO_3 , in EmmimNTf₂, at T 150 °C, and at [1,3-PDO]:[Ir] \cong 220.0: yields^a of **2**, selectivity towards **2**, **3**, **4**, and **5**, and TOF.

Entry	[1,3-PDO]:[Ir]	[Base]:[1,3-PDO]	% Yield ^a (2)	2	3	4	5	TOF ^b [s ⁻¹] ($\times 10^3$)
1	219.6	0.0310	73	77.6	9.4	6.6	6.4	7.41
2	219.9	0.0314	72	75.6	9.1	0.0	15.3	7.30
3	219.7	0.0314	71	70.4	14.6	1.2	13.8	7.21
4	221.1	0.0313	68	78.8	8.2	0.0	13.0	6.94
5	220.1	0.0304	74	76.2	9.2	0.0	14.6	7.54

All operations were carried out (a) at P = 0.35 bar; (b) with reaction time: 6 h; (c) at RPM: 1000. ^aCrude, isolated product. ^b TOF = n(product formed) / [n(catalyst) \times time].

Table S3. Recycling **1** as catalyst precursor for HTID of 1,3-PDO in the presence of K_2CO_3 , in EmmimNTf₂, at T 120 °C, and at [1,3-PDO]:[Ir] \cong 75.0: yields^a of **2**, selectivity towards **2**, **3**, **4**, and **5**, and TOF.

Entry	[1,3-PDO]:[Ir]	[Base]:[1,3-PDO]	% Yield ^a (2)	2	3	4	5	TOF ^b [s ⁻¹] ($\times 10^3$)
1	74.0	0.0308	72	71.2	13.5	10.8	4.4	2.48
2	73.6	0.0309	72	75.6	11.7	6.4	6.3	2.47
3	73.7	0.0311	79	74.1	15.3	2.5	8.1	2.68
4	73.8	0.0311	79	75.2	13.0	2.5	9.3	2.70
5	74.3	0.0311	78	76.2	11.8	1.3	10.6	2.68

All operations were carried out (a) at P = 0.35 bar; (b) with reaction time: 6 h; (c) at RPM: 1000. ^aCrude, isolated product. ^b TOF = n(product formed) / [n(catalyst) \times time].

Table S4. Recycling **1** as catalyst precursor for HTID of 1,3-PDO in the presence of K_2CO_3 , in N_{1,8,8,8}NTf₂, at T 150 °C, and at [1,3-PDO]:[Ir] \cong 220.0: yields^a of **2**, selectivity towards **2**, **3**, **4**, and **5**, and TOF.

Entry	[1,3-PDO]:[Ir]	[Base]:[1,3-PDO]	% Yield ^a (2)	2	3	4	5	TOF ^b [s ⁻¹] ($\times 10^3$)
1	221.4	0.0308	60	87.5	4.5	3.0	5.0	6.15
2	222.5	0.0305	48	78.9	9.5	1.3	10.2	4.95
3	222.8	0.0304	62	78.2	10.8	1.3	9.7	6.37
4	222.0	0.0305	56	76.6	10.6	1.3	11.5	5.73
5	222.1	0.0302	57	82.2	7.1	1.4	9.4	5.81

All operations were carried out (a) at P = 0.35 bar; (b) with reaction time: 6 h; (c) at RPM: 1000. ^aCrude, isolated product. ^b TOF = n(product formed) / [n(catalyst) \times time].

Table S5. Recycling **1** as catalyst precursor for HTID of 1,3-PDO in the presence of K_2CO_3 , in $N_{1,8,8,8}NTf_2$, at T 120 °C, and at [1,3-PDO]:[Ir] \cong 75.0: yields^a of **2**, selectivity towards **2**, **3**, **4**, and **5**, and TOF.

Entry	[1,3-PDO]:[Ir]	[Base]:[1,3-PDO]	% Yield ^a (2)	2	3	4	5	TOF ^b [s ⁻¹] ($\times 10^3$)
1	75.0	0.0308	59	73.2	15.1	8.7	3.0	2.04
2	74.8	0.0311	49	70.5	13.4	4.8	11.3	1.70
3	75.4	0.0307	67	76.6	10.6	1.3	11.5	2.35
4	75.0	0.0309	44	74.6	7.7	3.8	13.9	1.53
5	75.0	0.0305	60	76.0	6.5	2.6	14.9	2.10

All operations were carried out (a) at P = 0.35 bar; (b) with reaction time: 6 h; (c) at RPM: 1000. ^aCrude, isolated product. ^b TOF = n(product formed) / [n(catalyst) \times time].

Table S6. Recycling **1** as catalyst precursor for HTID of 1,3-PDO in the presence of K_2CO_3 , in $N_{1,8,8,8}NTf_2$, at T 150 °C, and at [1,3-PDO]:[Ir] \cong 75.0: yields^a of **2**, selectivity towards **2**, **3**, **4**, and **5**, and TOF.

Entry	[1,3-PDO]:[Ir]	[Base]:[1,3-PDO]	% Yield ^a (2)	2	3	4	5	TOF ^b [s ⁻¹] ($\times 10^3$)
1	77.0	0.0303	86	83.9	5.8	4.3	6.1	3.08
2	76.8	0.0311	22	78.4	4.1	1.3	16.2	0.77
3	76.9	0.0305	54	77.7	8.0	2.6	11.7	1.91
4	76.7	0.0312	65	75.5	9.1	2.6	12.9	2.30
5	76.3	0.0313	65	76.5	7.9	1.3	14.3	2.29
6	76.2	0.0307	66	79.3	8.2	2.7	9.8	2.34
7	76.0	0.0309	77	75.6	7.8	2.6	14.1	2.70
8	76.2	0.0311	65	73.1	11.3	4.9	10.6	2.29
9	75.3	0.0313	71	76.2	10.5	3.9	9.5	2.47
10	76.7	0.0309	58	73.4	8.9	3.7	14.0	2.05

All operations were carried out (a) at P = 0.35 bar; (b) with reaction time: 6 h; (c) at RPM: 1000. ^aCrude, isolated product. ^b TOF = n(product formed) / [n(catalyst) \times time].

Table S7. HTID of 1,3-PDO in the presence of **1** and K₂CO₃, at 120 °C, in EmmimNTf₂ and N_{1,8,8,8}NTf₂, and water, at [1,3-PDO]:[Ir] ≅ 75.0: selectivity towards **2**, **3**, **4**, and **5**.

Entry	Solvent	[1,3-PDO]:[Ir]	[Base]:[1,3-PDO]	2	3	4	5
1	EmmimNTf ₂	75.0	0.0303	83.4	5.8	0.0	10.8
2 ^a	N _{1,8,8,8} NTf ₂	74.0	0.0312	44.2	31.3	14.2	10.3
2 ^b	N _{1,8,8,8} NTf ₂	74.0	0.0312	73.2	6.3	1.2	19.3

All operations were carried out (a) at P = 1.00 bar; (b) with reaction time: 6 h; (c) at RPM: 1000. ^a Organic layer. ^b Water layer.

Experimental

Recycling Experiments

The recyclability of the catalyst precursor **1** was first tested on the addition of further aliquots of 1,3-PDO: the activity of the catalyst precursor quickly decreased and almost collapsed by the 2nd recycling run in N_{1,8,8,8}NTf₂, and the 4th recycling run in EmmimNTf₂. The recycling experiments were then repeated upon the addition of further aliquots of substrate and base.

HTID of 1,3-PDO in the presence of **1 and K₂CO₃, at 150 °C, in EmmimNTf₂ and N_{1,8,8,8}NTf₂, and at [1,3-PDO]:[Ir] \cong 75.0: recycling experiments.**

1,3-PDO (in Table S9 (for EmmimNTf₂) and Table S10 (for N_{1,8,8,8}NTf₂), see 1,3-PDO in entry 1), **1** (in Table S9 (for EmmimNTf₂) and Table S10 (for N_{1,8,8,8}NTf₂), see **1** in entry 1), K₂CO₃ (in Table S9 (for EmmimNTf₂) and Table S10 (for N_{1,8,8,8}NTf₂), see K₂CO₃ in entry 1), and EmmimNTf₂ (in Table S9, see EmmimNTf₂ in entry 1) or N_{1,8,8,8}NTf₂ (in Table S10, see N_{1,8,8,8}NTf₂ in entry 1), were mixed in a 50 mL round bottom flask connected, through a distillation condenser, to a 50 mL glass tube. The mixture was reacted at 150 °C, at a controlled pressure of *ca.* 0.35 bar, for six hours, stirring at 1000 rpm. The reaction product, a colourless liquid, was isolated by distillation, being collected, for the duration of the six hours reaction, in the collecting glass tube kept at *ca.* -196 °C (N₂ (l) bath). After separation from the minor water layer, the crude product (% yield (based on **2**): in Table S9 for EmmimNTf₂, and Table S10 for N_{1,8,8,8}NTf₂, see % Yield) was analysed by GC/MS (See Table S19 for EmmimNTf₂, and Table S20 for N_{1,8,8,8}NTf₂) and ¹H NMR (See Table S28 for EmmimNTf₂, and Table S29 for N_{1,8,8,8}NTf₂) spectroscopies. The reacted mixture, left in the 50 mL round bottom flask, was analysed by ¹H NMR spectroscopy. The following nine recycling experiments were carried out as follows: 1,3-PDO (in Table S9 (for EmmimNTf₂) and Table S10 (for N_{1,8,8,8}NTf₂), see 1,3-PDO in entries 2-10) and K₂CO₃ (in Table S9 (for EmmimNTf₂) and Table S10 (for N_{1,8,8,8}NTf₂), see K₂CO₃ in entries 2-10) were added to the reacted mixture resulting from the previous recycling experiment, in the 50 mL round bottom flask. The resulting mixture was reacted, and then analysed, as in the first cycle.

HTID of 1,3-PDO in the presence of **1 and K_2CO_3 , at 150 °C, in EmmimNTf₂ and N_{1,8,8,8}NTf₂, and at [1,3-PDO]:[Ir] \cong 220.0: recycling experiments.**

1,3-PDO (in Table S11 (for EmmimNTf₂) and Table S12 (for N_{1,8,8,8}NTf₂), see 1,3-PDO in entry 1), **1** (in Table S11 (for EmmimNTf₂) and Table S12 (for N_{1,8,8,8}NTf₂), see **1** in entry 1), K₂CO₃ (in Table S11 (for EmmimNTf₂) and Table S12 (for N_{1,8,8,8}NTf₂), see K₂CO₃ in entry 1), and EmmimNTf₂ (in Table S11, see EmmimNTf₂ in entry 1) or N_{1,8,8,8}NTf₂ (in Table S12, see N_{1,8,8,8}NTf₂ in entry 1), were mixed in a 50 mL round bottom flask and reacted at 150 °C, using the same glassware apparatus, procedure and conditions as those described above. The crude product (% yield (based on **2**): in Table S11 for EmmimNTf₂, and Table S12 for N_{1,8,8,8}NTf₂, see % Yield) was analysed by GC/MS (See Table S21 for EmmimNTf₂, and Table S22 for N_{1,8,8,8}NTf₂) and ¹H NMR (See Table S30 for EmmimNTf₂, and Table S31 for N_{1,8,8,8}NTf₂) spectroscopies. The reacted mixture, left in the 50 mL round bottom flask, was analysed by ¹H NMR spectroscopy. The next four recycling experiments were carried out as follows: 1,3-PDO (in Table S11 (for EmmimNTf₂) and Table S12 (for N_{1,8,8,8}NTf₂), see 1,3-PDO in entries 2-5) and K₂CO₃ (in Table S11 (for EmmimNTf₂) and Table S12 (for N_{1,8,8,8}NTf₂), see K₂CO₃ in entries 2-5) were added to the reacted mixture resulting from the previous recycling experiment, in the 50 mL round bottom flask. The resulting mixture was reacted, and then analysed, as in the first cycle.

HTID of 1,3-PDO in the presence of **1 and K_2CO_3 , at 120 °C, in EmmimNTf₂ and N_{1,8,8,8}NTf₂, and at [1,3-PDO]:[Ir] \cong 75.0: recycling experiments.**

1,3-PDO (in Table S13 (for EmmimNTf₂) and Table S14 (for N_{1,8,8,8}NTf₂), see 1,3-PDO in entry 1), **1** (in Table S13 (for EmmimNTf₂) and Table S14 (for N_{1,8,8,8}NTf₂), see **1** in entry 1), K₂CO₃ (in Table S13 (for EmmimNTf₂) and Table S14 (for N_{1,8,8,8}NTf₂), see K₂CO₃ in entry 1), and EmmimNTf₂ (in Table S13, see EmmimNTf₂ in entry 1) or N_{1,8,8,8}NTf₂ (in Table S14, see N_{1,8,8,8}NTf₂ in entry 1), were mixed in a 50 mL round bottom flask and reacted at 120 °C, using the same glassware apparatus, procedure and conditions as those described above. The crude product (% yield (based on **2**): in Table S13 for EmmimNTf₂, and Table S14 for N_{1,8,8,8}NTf₂, see % Yield) was analysed by GC/MS (See Table S23 for EmmimNTf₂, and Table S24 for N_{1,8,8,8}NTf₂) and ¹H NMR (See Table S32 for EmmimNTf₂, and Table S33 for N_{1,8,8,8}NTf₂) spectroscopies. The reacted mixture, left in the 50 mL round bottom flask, was analysed by ¹H NMR spectroscopy. The next four recycling experiments were carried out as follows: 1,3-PDO (in Table S13 (for EmmimNTf₂) and Table S14 (for N_{1,8,8,8}NTf₂), see 1,3-PDO in entries 2-5) and K₂CO₃ (in Table S13 (for EmmimNTf₂) and Table S14 (for

$N_{1,8,8,8}NTf_2$), see K_2CO_3 in entries 2-5) were added to the reacted mixture resulting from the previous recycling experiment, in the 50 mL round bottom flask. The resulting mixture was reacted, and then analysed, as in the first cycle.

HTID of 1,3-PDO in the presence of **1 and K_2CO_3 , in EmmimNTf₂: mercury poisoning test of the iridium precatalyst **1**.**

1,3-PDO (1.2471 g, 0.0161 mol), **1** (0.0445 g, 0.078 mmol), K_2CO_3 (0.0695 g, 0.500 mmol), EmmimNTf₂ (2.8138 g, 0.0069 mol), and mercury (0.4870 g) were mixed in a 50 mL round bottom flask and reacted at 150 °C (Table S15), using the same glassware apparatus, procedure and conditions as those described above. The crude product (0.7146 g, % yield (based on **2**): 77 %) (Table S15) was analysed by GC/MS (Table S25) and ¹H NMR (Table S34) spectroscopies.

HTID of 1,3-PDO in the presence of **1 and K_2CO_3 , at 120 °C, in EmmimNTf₂ and $N_{1,8,8,8}NTf_2$, and water, at [1,3-PDO]:[Ir] \cong 75.0.**

1,3-PDO (in Table S16, see 1,3-PDO in entry 1 for EmmimNTf₂ and entry 2 for $N_{1,8,8,8}NTf_2$), **1** (in Table S16, see **1** in entry 1 for EmmimNTf₂ and entry 2 for $N_{1,8,8,8}NTf_2$), K_2CO_3 (in Table S16, see K_2CO_3 in entry 1 for EmmimNTf₂ and entry 2 for $N_{1,8,8,8}NTf_2$), EmmimNTf₂ (in Table S16, see Solvent in entry 1) or $N_{1,8,8,8}NTf_2$ (in Table S16, see Solvent in entry 2), and water (in Table S16, see H₂O in entry 1 for EmmimNTf₂ and entry 2 for $N_{1,8,8,8}NTf_2$) were mixed in a 50 mL round bottom flask. The mixture was reacted at 120 °C, at atmospheric pressure, for six hours, stirring at 1000 rpm. The reaction product, a colourless liquid, was isolated by distillation, being collected, for the duration of the six hours reaction, in the collecting glass tube kept at *ca.* -196 °C (N₂ (l) bath). The crude product organic and water layers were separated. Significant amounts of water were collected when using both EmmimNTf₂ and $N_{1,8,8,8}NTf_2$, preventing any evaluation of the % yield of the crude product; mass balance was evaluated *via* GC and NMR spectroscopy (Table S35). The organic and water layers were then analysed by GC/MS (See entry 1 for EmmimNTf₂, and entry 2 for $N_{1,8,8,8}NTf_2$, in Table S26) and ¹H NMR (See entry 1 for EmmimNTf₂, and entry 2 for $N_{1,8,8,8}NTf_2$, in Table S35) spectroscopies.

Table S8. HTID of 1,3-PDO in the presence of **1** and a base, in ionic liquids: experimental data for screening conditions experiments. (Entries 1-32 correspond to those in Table 1.).

Entry	1,3-PDO [g]	n(1,3-PDO) [mol]	1 [g]	n(1) [mmol]	Base	Base [g]	n(Base) [mmol]	Solvent	Solvent [g]	n(Solvent) [mol]	T [°C]	% Yield ^a (2)
1	1.2301	0.0158	0.1210	0.212	K ₂ CO ₃	0.0683	0.492	N _{1,8,8,8} NTf ₂	4.6173	0.0071	150	84
2	1.2205	0.0157	0.1227	0.215	K ₂ CO ₃	0.0678	0.488	N _{1,8,8,8} NTf ₂	4.6085	0.0071	120	60
3	1.2451	0.0160	0.1205	0.211	K ₂ CO ₃	0.0672	0.484	N _{1,8,8,8} NTf ₂	4.6145	0.0071	100	27
4	1.2352	0.0159	0.1203	0.210	K ₂ CO ₃	0.0688	0.495	N _{1,8,8,8} NTf ₂	4.6166	0.0071	80	1
5	1.2152	0.0157	0.1221	0.214	K ₂ CO ₃	0.0670	0.482	N _{1,8,8,8} NTf ₂	4.6747	0.0072	150	84
6	1.2190	0.0157	0.0907	0.159	K ₂ CO ₃	0.0673	0.485	N _{1,8,8,8} NTf ₂	4.6828	0.0072	150	69
7	1.2216	0.0157	0.0409	0.072	K ₂ CO ₃	0.0662	0.477	N _{1,8,8,8} NTf ₂	4.6651	0.0072	150	51
8	1.2145	0.0156	0.0180	0.031	K ₂ CO ₃	0.0674	0.485	N _{1,8,8,8} NTf ₂	4.6729	0.0072	150	6
9	1.2114	0.0156	0.0411	0.072	K ₂ CO ₃	0.0684	0.492	N _{1,8,8,8} NTf ₂	4.6120	0.0071	180	49
10	1.2112	0.0156	0.1212	0.212	KOH	0.0561	0.850	N _{1,8,8,8} NTf ₂	4.6065	0.0071	150	78
11	1.2280	0.0158	0.1209	0.212	KOH	0.0560	0.848	N _{1,8,8,8} NTf ₂	4.6050	0.0071	100	11
12	1.2178	0.0157	0.0410	0.072	KOH	0.0560	0.848	N _{1,8,8,8} NTf ₂	4.6099	0.0071	150	62
13	1.2247	0.0158	0.0413	0.072	KOH	0.0516	0.782	N _{1,8,8,8} NTf ₂	4.6228	0.0071	100	2
14	1.2333	0.0159	0.0413	0.072	K ₂ CO ₃	0.3011	2.168	N _{1,8,8,8} NTf ₂	4.6053	0.0071	150	29
15	1.2326	0.0159	0.0416	0.073	K ₂ CO ₃	0.6094	4.387	N _{1,8,8,8} NTf ₂	4.6032	0.0071	150	20
16	1.2249	0.0158	0.0435	0.076	CsCO ₃	0.1652	0.507	N _{1,8,8,8} NTf ₂	4.6050	0.0071	150	17
17	1.2134	0.0156	No catalyst	/	K ₂ CO ₃	0.0678	0.488	N _{1,8,8,8} NTf ₂	4.6130	0.0071	150	/
18	1.2212	0.0157	0.0407	0.071	No base	/	/	N _{1,8,8,8} NTf ₂	4.6037	0.0071	150	/
19	1.2374	0.0159	0.0402	0.070	K ₂ CO ₃	0.0689	0.496	No IL	/	/	150	69
20	1.2331	0.0159	0.1207	0.211	K ₂ CO ₃	0.0682	0.491	EmmimNTf ₂	2.8107	0.0069	180	85
21	1.2255	0.0158	0.1202	0.210	K ₂ CO ₃	0.0690	0.497	EmmimNTf ₂	2.8906	0.0071	150	78
22	1.2418	0.0160	0.1209	0.212	K ₂ CO ₃	0.0683	0.492	EmmimNTf ₂	2.8879	0.0071	120	74
23	1.2314	0.0159	0.1213	0.212	K ₂ CO ₃	0.0685	0.493	EmmimNTf ₂	2.9095	0.0072	100	60
24	1.2218	0.0157	0.1202	0.210	K ₂ CO ₃	0.0682	0.491	EmmimNTf ₂	2.8713	0.0071	80	1
25	1.2330	0.0159	0.0409	0.072	K ₂ CO ₃	0.0692	0.498	EmmimNTf ₂	2.889	0.0071	180	62
26	1.2176	0.0157	0.0408	0.071	K ₂ CO ₃	0.0686	0.494	EmmimNTf ₂	2.8985	0.0072	150	70
27	1.2485	0.0161	0.0407	0.071	K ₂ CO ₃	0.0680	0.490	EmmimNTf ₂	2.9036	0.0072	120	51
28	1.2344	0.0159	0.0402	0.070	KOH	0.0582	0.882	EmmimNTf ₂	2.8618	0.0071	150	54
29	1.2199	0.0157	0.1205	0.211	KOH	0.0560	0.848	EmmimNTf ₂	2.8818	0.0071	80	1
30	1.2356	0.0159	0.0413	0.072	CsCO ₃	0.1621	0.497	EmmimNTf ₂	2.8904	0.0071	150	67
31	1.2565	0.0162	0.1209	0.212	K ₂ CO ₃	0.0706	0.508	1,3-PDO	4.4294	0.0582	150	290 ^b
32	1.2543	0.0162	0.1197	0.209	K ₂ CO ₃	0.0695	0.500	1,3-PDO	2.0030	0.0263	150	197 ^b

All operations were carried out (a) at P = 0.35 bar; (b) with reaction time: 6 h; (c) at RPM: 1000. ^a Crude, isolated product. ^b In entries 31 and 32, 1,3-PDO was used as both the substrate and the solvent.

Table S9. HTID of 1,3-PDO in the presence of **1** and K₂CO₃, in EmmimNTf₂, at T 150 °C, and at [1,3-PDO]:[Ir] ≅ 75.0: experimental data for recycling experiments. (Entries 1-10 correspond to those in Table S1.).

Entry	1,3-PDO [g]	n(1,3-PDO) [mol]	1 [g]	n(1) [mmol]	K ₂ CO ₃ [g]	n(K ₂ CO ₃) [mmol]	EmmimNTf ₂ [g]	n(EmmimNTf ₂) [mol]	% Yield ^a (2)
1	1.2654	0.0163	0.1202	0.210	0.0686	0.494	2.8794	0.0071	82
2	1.2496	0.0161	-	-	0.0695	0.500	-	-	94
3	1.2563	0.0162	-	-	0.0696	0.501	-	-	77
4	1.2467	0.0161	-	-	0.0682	0.491	-	-	99
5	1.2528	0.0162	-	-	0.0682	0.491	-	-	99
6	1.2471	0.0161	-	-	0.0685	0.493	-	-	97
7	1.2556	0.0162	-	-	0.0688	0.495	-	-	89
8	1.2395	0.0157	-	-	0.0679	0.489	-	-	79
9	1.2424	0.0160	-	-	0.0685	0.493	-	-	80
10	1.2574	0.0162	-	-	0.0694	0.500	-	-	75

All operations were carried out (a) at P = 0.35 bar; (b) with reaction time: 6 h; (c) at RPM: 1000. ^a Crude, isolated product.

Table S10. HTID of 1,3-PDO in the presence of **1** and K₂CO₃, in N_{1,8,8,8}NTf₂, at T 150 °C, and at [1,3-PDO]:[Ir] ≅ 75.0: experimental data for recycling experiments. (Entries 1-10 correspond to those in Table S6.).

Entry	1,3-PDO [g]	n(1,3-PDO) [mol]	1 [g]	n(1) [mmol]	K ₂ CO ₃ [g]	n(K ₂ CO ₃) [mmol]	N _{1,8,8,8} NTf ₂ [g]	n(N _{1,8,8,8} NTf ₂) [mol]	% Yield ^a (2)
1	1.2604	0.0162	0.1205	0.211	0.0683	0.492	4.6080	0.0071	86
2	1.2572	0.0162	-	-	0.0700	0.504	-	-	22
3	1.2585	0.0162	-	-	0.0686	0.494	-	-	54
4	1.2547	0.0162	-	-	0.0701	0.505	-	-	65
5	1.2492	0.0161	-	-	0.0700	0.504	-	-	65
6	1.2471	0.0161	-	-	0.0686	0.494	-	-	66
7	1.2444	0.0160	-	-	0.0687	0.495	-	-	77
8	1.2467	0.0161	-	-	0.0693	0.499	-	-	65
9	1.2329	0.0159	-	-	0.0691	0.497	-	-	71
10	1.2557	0.0162	-	-	0.0694	0.500	-	-	58

All operations were carried out (a) at P = 0.35 bar; (b) with reaction time: 6 h; (c) at RPM: 1000. ^a Crude, isolated product.

Table S11. HTID of 1,3-PDO in the presence of **1** and K₂CO₃, in EmmimNTf₂, at T 150 °C, and at [1,3-PDO]:[Ir] ≅ 220.0: experimental data for recycling experiments. (Entries 1-5 correspond to those in Table S2.).

Entry	1,3-PDO [g]	n(1,3-PDO) [mol]	1 [g]	n(1) [mmol]	K ₂ CO ₃ [g]	n(K ₂ CO ₃) [mmol]	EmmimNTf ₂ [g]	n(EmmimNTf ₂) [mol]	% Yield ^a (2)
1	1.2408	0.0160	0.0416	0.073	0.0688	0.495	2.8074	0.0069	73
2	1.2425	0.0160	-	-	0.0698	0.503	-	-	72
3	1.2414	0.0160	-	-	0.0698	0.503	-	-	71
4	1.2493	0.0161	-	-	0.0700	0.504	-	-	68
5	1.2440	0.0160	-	-	0.0677	0.487	-	-	74

All operations were carried out (a) at P = 0.35 bar; (b) with reaction time: 6 h; (c) at RPM: 1000. ^a Crude, isolated product.

Table S12. HTID of 1,3-PDO in the presence of **1** and K₂CO₃, in N_{1,8,8,8}NTf₂, at T 150 °C, and at [1,3-PDO]:[Ir] ≅ 220.0: experimental data for recycling experiments. (Entries 1-5 correspond to those in Table S4.).

Entry	1,3-PDO [g]	n(1,3-PDO) [mol]	1 [g]	n(1) [mmol]	K ₂ CO ₃ [g]	n(K ₂ CO ₃) [mmol]	N _{1,8,8,8} NTf ₂ [g]	n(N _{1,8,8,8} NTf ₂) [mol]	% Yield ^a (2)
1	1.2449	0.0160	0.0414	0.072	0.0685	0.493	4.6054	0.0071	60
2	1.2512	0.0161	-	-	0.0682	0.491	-	-	48
3	1.2530	0.0161	-	-	0.0682	0.491	-	-	62
4	1.2486	0.0161	-	-	0.0681	0.490	-	-	56
5	1.2492	0.0161	-	-	0.0676	0.487	-	-	57

All operations were carried out (a) at P = 0.35 bar; (b) with reaction time: 6 h; (c) at RPM: 1000. ^a Crude, isolated product.

Table S13. HTID of 1,3-PDO in the presence of **1** and K₂CO₃, in EmmimNTf₂, at T 120 °C, and at [1,3-PDO]:[Ir] ≅ 75.0: experimental data for recycling experiments. (Entries 1-5 correspond to those in Table S3.).

Entry	1,3-PDO [g]	n(1,3-PDO) [mol]	1 [g]	n(1) [mmol]	K ₂ CO ₃ [g]	n(K ₂ CO ₃) [mmol]	EmmimNTf ₂ [g]	n(EmmimNTf ₂) [mol]	% Yield ^a (2)
1	1.2420	0.0160	0.1235	0.216	0.0685	0.493	2.8048	0.0069	72
2	1.2349	0.0159	-	-	0.0682	0.491	-	-	72
3	1.2368	0.0159	-	-	0.0689	0.496	-	-	79
4	1.2389	0.0160	-	-	0.0689	0.496	-	-	79
5	1.2473	0.0161	-	-	0.0694	0.500	-	-	78

All operations were carried out (a) at P = 0.35 bar; (b) with reaction time: 6 h; (c) at RPM: 1000. ^a Crude, isolated product.

Table S14. HTID of 1,3-PDO in the presence of **1** and K₂CO₃, in N_{1,8,8,8}NTf₂, at T 120 °C, and at [1,3-PDO]:[Ir] ≅ 75.0: experimental data for recycling experiments. (Entries 1-5 correspond to those in Table S5.).

Entry	1,3-PDO [g]	n(1,3-PDO) [mol]	1 [g]	n(1) [mmol]	K ₂ CO ₃ [g]	n(K ₂ CO ₃) [mmol]	N _{1,8,8,8} NTf ₂ [g]	n(N _{1,8,8,8} NTf ₂) [mol]	% Yield ^a (2)
1	1.2437	0.0160	0.1221	0.214	0.0686	0.494	4.6033	0.0071	59
2	1.2401	0.0160	-	-	0.0690	0.497	-	-	49
3	1.2499	0.0161	-	-	0.0686	0.494	-	-	67
4	1.2446	0.0160	-	-	0.0689	0.496	-	-	44
5	1.2438	0.0160	-	-	0.0679	0.498	-	-	60

All operations were carried out (a) at P = 0.35 bar; (b) with reaction time: 6 h; (c) at RPM: 1000. ^a Crude, isolated product.

Table S15. Mercury poisoning test of the iridium precatalyst in HTID of 1,3-PDO in the presence of **1** and K₂CO₃, in EmmimNTf₂, at T 150 °C, and at [1,3-PDO]:[Ir] ≅ 220.0: experimental data.

1,3-PDO [g]	n(1,3-PDO) [mol]	1 [g]	n(1) [mmol]	K ₂ CO ₃ [g]	n(K ₂ CO ₃) [mmol]	EmmimNTf ₂ [g]	n(EmmimNTf ₂) [mol]	Hg [g]	% Yield ^a (2)
1.2471	0.0161	0.0445	0.078	0.0695	0.500	2.8138	0.0069	0.4870	77

The reaction was carried out (a) at P = 0.35 bar; (b) with reaction time: 6 h; (c) at RPM: 1000. ^a Crude, isolated product.

Table S16. HTID of 1,3-PDO in the presence of **1** and K₂CO₃, in EmmimNTf₂ and N_{1,8,8}NTf₂, and water, at T 120 °C, and at [1,3-PDO]:[Ir] ≅ 75.0: experimental data.

Entry	1,3-PDO [g]	n(1,3-PDO) [mol]	1 [g]	n(1) [mmol]	K ₂ CO ₃ [g]	n(K ₂ CO ₃) [mmol]	Solvent	Solvent [g]	n(Solvent) [mol]	H ₂ O [g]
1	1.2655	0.0163	0.1242	0.217	0.0686	0.494	EmmimNTf ₂	2.8809	0.0071	3.0338
2	1.2505	0.0161	0.1244	0.218	0.0699	0.503	N _{1,8,8} NTf ₂	4.6113	0.0071	3.0124

All operations were carried out (a) at P = 1.00 bar; (b) with reaction time: 6 h; (c) at RPM: 1000.

GC/MS analysis of reaction product solutions.**GC/MS analysis of reaction product solutions: CH₃CH₂CH₂OH (5) / CDCl₃ / CH₃OH calibration.**

Six solutions of **5** and CDCl₃ (internal standard) in CH₃OH were prepared (Table S17): **5** was first dissolved in 1.0 mL of CH₃OH; CDCl₃ (**6**) was then added. The resulting solutions were analysed by GC/MS spectroscopy. GC/MS spectroscopic data (A₅ and A₆) for each solution are reported in Table S17. The following calibration curve was attained (Figure S9):

$$y = 0.4449x - 0.0345 \quad (R^2 = 0.9938) \quad (x = C_5/C_6, y = A_5/A_6). \quad (\text{Eq. S1})$$

Table S17. GC/MS **5** / CDCl₃ / CH₃OH calibration: experimental and GC/MS data for the **5** / CDCl₃ solutions in CH₃OH.

Solution	5 [g]	6 [g]	CH ₃ OH [mL]	C ₅ [M]	C ₆ [M]	C ₅ /C ₆	A ₅	A ₆	A ₅ /A ₆
1	0.0008	0.0042	1.0	0.0129	0.0344	0.3738	1013034.22	7673580.57	0.1320
2	0.0019	0.0042	1.0	0.0305	0.0344	0.8878	2759672.87	7271535.13	0.3795
3	0.0017	0.0052	1.0	0.0273	0.0425	0.6416	2054314.61	8411117.17	0.2442
4	0.0025	0.0045	1.0	0.0401	0.0368	1.0903	3350151.93	7596100.42	0.4410
5	0.0031	0.0045	1.0	0.0497	0.0368	1.3520	3873803.95	6690433.20	0.5790
6	0.0029	0.0046	1.0	0.0465	0.0376	1.2372	3757553.96	7497487.91	0.5012

6 (Assay: 99.0 %): d, 1.500 g/mL; FW, 120.38 g/mol. **5** (Assay: 97.0 %): d, 0.804 g/mL; FW, 60.10 g/mol.

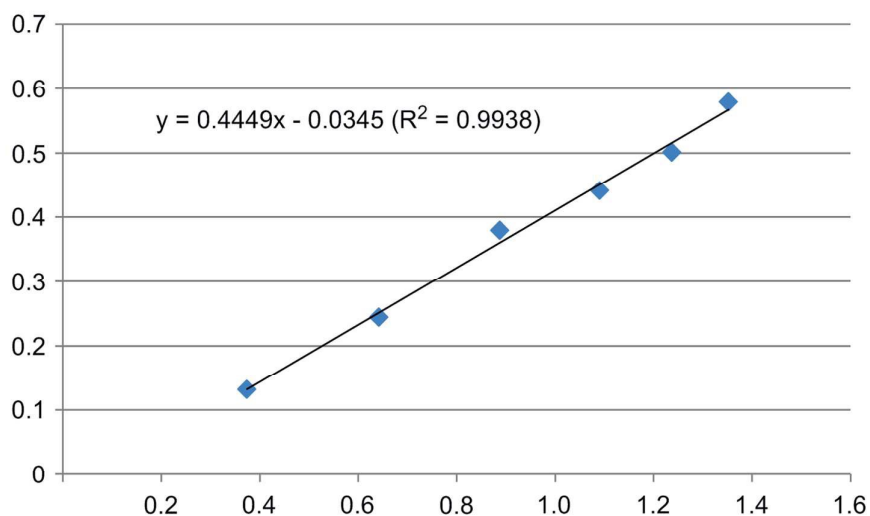


Figure S9. GC/MS **5** / CDCl₃ / CH₃OH calibration curve (where x = C₅/C₆, y = A₅/A₆).

GC/MS analysis of reaction product solutions: general methodology for screening conditions experiments, and catalyst recycling experiments.

A known amount of the reaction product solutions (**PS** in tables S18, S19, S20, S21, S22, S23, S24, S25, S26) was first dissolved in 1.0 mL of CH₃OH; CDCl₃ (**6** in tables S18, S19, S20, S21, S22, S23, S24, S25, S26) was then added. The resulting solutions were analysed by GC/MS spectroscopy. GC/MS spectroscopic data (**A₅** and **A₆**) for each solution are reported in tables S18, S19, S20, S21, S22, S23, S24, S25, S26. [**5**] (**C₅**) was then calculated using equation Eq. S1. Entries 1-32 in Table S18 correspond to entries 1-32 in Table 1, entries 1-10 in Table S19 correspond to entries 1-10 in Table S1, entries 1-10 in Table S20 correspond to entries 1-10 in Table S6, entries 1-5 in Table S21 correspond to entries 1-5 in Table S2, entries 1-5 in Table S22 correspond to entries 1-5 in Table S4, entries 1-5 in Table S23 correspond to entries 1-5 in Table S3, entries 1-5 in Table S24 correspond to entries 1-5 in Table S5, entries 1 and 2 in Table S26 correspond to entries 1 and 2 in Table S7.

Table S18. GC/MS analysis of the product solutions of HTID of 1,3-PDO in the presence of **1** and a base, in ionic liquids: experimental and GC/MS data for screening conditions experiments.

Entry	PS [g]	6 [g]	CH ₃ OH [mL]	C ₆ [M]	A ₅	A ₆	A ₅ /A ₆	C ₅ [M]
1	0.0084	0.0081	1.0	0.0663	102324.62	2985700.37	0.0343	0.0102
2	0.0061	0.0073	1.0	0.0597	272351.22	9837361.45	0.0277	0.0083
3	0.0073	0.0075	1.0	0.0614	155214.08	10751355.50	0.0144	0.0067
4	0.0076	0.0073	1.0	0.0597	517000.97	9632947.61	0.0537	0.0118
5	0.0126	0.0055	1.0	0.0451	1233902.77	7884826.09	0.1565	0.0193
6	0.0069	0.0031	1.0	0.0254	325930.45	5320797.82	0.0613	0.0055
7	0.0107	0.0058	1.0	0.0475	761932.58	7709523.86	0.0988	0.0142
8	0.0046	0.0038	1.0	0.0312	319835.37	11740461.92	0.0272	0.0043
9	0.0078	0.0077	1.0	0.0630	340378.24	10824496.75	0.0314	0.0093
10	0.0132	0.0076	1.0	0.0622	1358672.55	10444426.44	0.1301	0.0230
11	0.0079	0.0079	1.0	0.0646	497190.53	10635989.57	0.0467	0.0118
12	0.0135	0.0073	1.0	0.0597	988651.28	12438588.77	0.0795	0.0153
13	0.0047	0.0084	1.0	0.0687	283091.78	8224857.12	0.0344	0.0106
14	0.0124	0.0075	1.0	0.0614	1763943.87	10441529.91	0.1689	0.0281
15	0.0126	0.0072	1.0	0.0589	1704760.52	10188912.33	0.1673	0.0267
16	0.0092	0.0081	1.0	0.0663	146135.99	3388220.27	0.0431	0.0115
17	-	-	-	-	-	-	-	-
18	-	-	-	-	-	-	-	-
19	0.0072	0.0082	1.0	0.0671	66107.31	3219458.48	0.0205	0.0082
20	0.0079	0.0073	1.0	0.0597	380637.06	7422572.89	0.0513	0.0115
21	0.0141	0.0074	1.0	0.0606	1154804.05	10112015.19	0.1142	0.0202
22	0.0069	0.0082	1.0	0.0671	56773.97	3107328.44	0.0183	0.0079
23	0.0128	0.0079	1.0	0.0646	584091.88	10134934.91	0.0576	0.0133
24	0.0059	0.0069	1.0	0.0565	196051.85	10050407.50	0.0195	0.0068
25	0.0075	0.0075	1.0	0.0614	491145.68	10575376.42	0.0464	0.0111
26	0.0072	0.0083	1.0	0.0679	477423.54	11598509.99	0.0412	0.0115
27	0.0063	0.0078	1.0	0.0638	^a	7891567.82	^a	^a
28	0.0088	0.0088	1.0	0.0719	131971.90	3079263.98	0.0429	0.0125
29	0.0061	0.0083	1.0	0.0679	877749.49	10619803.41	0.0827	0.0178
30	0.0077	0.0075	1.0	0.0614	531112.79	7067782.58	0.0751	0.0151
31	0.0070	0.0079	1.0	0.0646	172080.59	8907511.33	0.0193	0.0078
32	0.0078	0.0072	1.0	0.0589	371426.13	9147734.29	0.0406	0.0099

6 (Assay: 99.0 %): d, 1.500 g/mL; FW, 120.38 g/mol. ^a The intensity of the GC peak due to **5** was so little that no reliable integration could be obtained.

Table S19. GC/MS analysis of the product solutions of HTID of 1,3-PDO in the presence of **1** and K₂CO₃, in EmmimNTf₂, at T 150 °C, and at [1,3-PDO]:[Ir] ≅ 75.0: experimental and GC/MS data for recycling experiments.

Entry	PS [g]	6 [g]	CH ₃ OH [mL]	C ₆ [M]	A ₅	A ₆	A ₅ /A ₆	C ₅ [M]
1	0.0075	0.0072	1.0	0.0589	499200.96	6862519.11	0.0727	0.0142
2	0.0041	0.0071	1.0	0.0581	609014.43	6144735.96	0.0991	0.0174
3	0.0085	0.0069	1.0	0.0565	1081598.64	5667770.54	0.1908	0.0286
4	0.0044	0.0076	1.0	0.0622	573213.53	5929776.77	0.0967	0.0183
5	0.0044	0.0079	1.0	0.0646	588508.24	6243740.77	0.0943	0.0187
6	0.0037	0.0065	1.0	0.0532	534301.84	5927639.67	0.0901	0.0149
7	0.0034	0.0074	1.0	0.0606	454281.16	5780631.10	0.0786	0.0154
8	0.0042	0.0064	1.0	0.0524	546125.4	5351376.99	0.1021	0.0161
9	0.0041	0.0077	1.0	0.0630	497472.57	5820209.99	0.0855	0.0170
10	0.0037	0.0071	1.0	0.0581	438920.97	5699379.73	0.0770	0.0145

6 (Assay: 99.0 %): d, 1.500 g/mL; FW, 120.38 g/mol.

Table S20. GC/MS analysis of the product solutions of HTID of 1,3-PDO in the presence of **1** and K₂CO₃, in N_{1,8,8,8}NTf₂, at T 150 °C, and at [1,3-PDO]:[Ir] ≅ 75.0: experimental and GC/MS data for recycling experiments.

Entry	PS [g]	6 [g]	CH ₃ OH [mL]	C ₆ [M]	A ₅	A ₆	A ₅ /A ₆	C ₅ [M]
1	0.0069	0.0066	1.0	0.0540	55277.21	6945973.55	0.0080	0.0051
2	0.0083	0.0074	1.0	0.0606	801444.24	6168126.25	0.1299	0.0224
3	0.0079	0.0067	1.0	0.0549	537506.57	5115698.34	0.1051	0.0172
4	0.0082	0.0066	1.0	0.0540	696444.39	4478957.85	0.1555	0.0231
5	0.0083	0.0073	1.0	0.0597	621060.09	5512967.13	0.1127	0.0197
6	0.0085	0.0069	1.0	0.0565	614588.57	5989198.85	0.1026	0.0174
7	0.0072	0.0065	1.0	0.0532	531945.86	5468938.47	0.0973	0.0157
8	0.0070	0.0066	1.0	0.0540	535487.16	5252853.60	0.1019	0.0165
9	0.0087	0.0083	1.0	0.0679	586837.64	5981514.96	0.0981	0.0202
10	0.0082	0.0070	1.0	0.0573	581773.19	5440390.86	0.1069	0.0182

6 (Assay: 99.0 %): d, 1.500 g/mL; FW, 120.38 g/mol.

Table S21. GC/MS analysis of the product solutions of HTID of 1,3-PDO in the presence of **1** and K_2CO_3 , in $EmmimNTf_2$, at T 150 °C, and at [1,3-PDO]:[Ir] \cong 220.0: experimental and GC/MS data for recycling experiments.

Entry	PS [g]	6 [g]	CH ₃ OH [mL]	C ₆ [M]	A ₅	A ₆	A ₅ /A ₆	C ₅ [M]
1	0.0089	0.0089	1.0	0.0728	256627.04	5177945.44	0.0496	0.0137
2	0.0103	0.0080	1.0	0.0654	619235.11	4961043.67	0.1248	0.0234
3	0.0096	0.0072	1.0	0.0589	542152.46	5032852.02	0.1077	0.0188
4	0.0095	0.0092	1.0	0.0752	514523.63	5198450.26	0.0990	0.0225
5	0.0091	0.0075	1.0	0.0614	511619.73	4911556.16	0.1042	0.0191

6 (Assay: 99.0 %): d, 1.500 g/mL; FW, 120.38 g/mol.

Table S22. GC/MS analysis of the product solutions of HTID of 1,3-PDO in the presence of **1** and K_2CO_3 , in $N_{1,8,8}NTf_2$, at T 150 °C, and at [1,3-PDO]:[Ir] \cong 220.0: experimental and GC/MS data for recycling experiments.

Entry	PS [g]	6 [g]	CH ₃ OH [mL]	C ₆ [M]	A ₅	A ₆	A ₅ /A ₆	C ₅ [M]
1	0.0095	0.0078	1.0	0.0638	156254.34	5055833.22	0.0309	0.0093
2	0.0090	0.0083	1.0	0.0679	343229.67	4614569.99	0.0744	0.0166
3	0.0088	0.0085	1.0	0.0695	370953.58	4976594.47	0.0745	0.0170
4	0.0090	0.0087	1.0	0.0711	472525.88	5035978.23	0.0938	0.0205
5	0.0088	0.0080	1.0	0.0654	346394.90	5192949.88	0.0667	0.0148

6 (Assay: 99.0 %): d, 1.500 g/mL; FW, 120.38 g/mol.

Table S23. GC/MS analysis of the product solutions of HTID of 1,3-PDO in the presence of **1** and K₂CO₃, in EmmimNTf₂, at T 120 °C, and at [1,3-PDO]:[Ir] ≅ 75.0: experimental and GC/MS data for recycling experiments.

Entry	PS [g]	6 [g]	CH ₃ OH [mL]	C ₆ [M]	A ₅	A ₆	A ₅ /A ₆	C ₅ [M]
1	0.0090	0.0086	1.0	0.0703	83236.32	3498817.23	0.0238	0.0092
2	0.0086	0.0079	1.0	0.0646	117556.99	3074175.20	0.0382	0.0105
3	0.0079	0.0090	1.0	0.0736	125514.35	3144128.39	0.0399	0.0122
4	0.0081	0.0084	1.0	0.0687	154807.01	3218303.41	0.0481	0.0127
5	0.0080	0.0080	1.0	0.0654	194239.29	2883570.49	0.0674	0.0149

6 (Assay: 99.0 %): d, 1.500 g/mL; FW, 120.38 g/mol.

Table S24. GC/MS analysis of the product solutions of HTID of 1,3-PDO in the presence of **1** and K₂CO₃, in N_{1,8,8,8}NTf₂, at T 120 °C, and at [1,3-PDO]:[Ir] ≅ 75.0: experimental and GC/MS data for recycling experiments.

Entry	PS [g]	6 [g]	CH ₃ OH [mL]	C ₆ [M]	A ₅	A ₆	A ₅ /A ₆	C ₅ [M]
1	0.0086	0.0071	1.0	0.0581	101789.13	4800306.01	0.0212	0.0072
2	0.0081	0.0070	1.0	0.0573	466601.36	4898414.03	0.0953	0.0167
3	0.0070	0.0071	1.0	0.0581	425913.09	5024981.20	0.0848	0.0155
4	0.0049	0.0076	1.0	0.0622	310619.81	4970078.85	0.0625	0.0135
5	0.0074	0.0076	1.0	0.0622	511044.48	4660797.72	0.1096	0.0201

6 (Assay: 99.0 %): d, 1.500 g/mL; FW, 120.38 g/mol.

Table S25. Mercury poisoning test of the iridium precatalyst in HTID of 1,3-PDO in the presence of **1** and K₂CO₃, in EmmimNTf₂: experimental and GC/MS data.

PS [g]	6 [g]	CH ₃ OH [mL]	C ₆ [M]	A ₅	A ₆	A ₅ /A ₆	C ₅ [M]
0.0066	0.0091	1.0	0.0744	24321.41	3183422.67	0.0076	0.0070

6 (Assay: 99.0 %): d, 1.500 g/mL; FW, 120.38 g/mol.

Table S26. GC/MS analysis of the product solutions of HTID of 1,3-PDO in the presence of **1** and K₂CO₃, at 120 °C, in EmmimNTf₂ and N_{1,8,8,8}NTf₂, and water, at [1,3-PDO]:[Ir] ≅ 75.0: experimental and GC/MS data.

Entry	PS [g]	6 [g]	CH ₃ OH [mL]	C ₆ [M]	A ₅	A ₆	A ₅ /A ₆	C ₅ [M]
1	0.0116	0.0087	1.0	0.0711	19457.83	2860426.88	0.0068	0.0065
2 ^a	0.0046	0.0088	1.0	0.0719	71335.84	2925316.90	0.0244	0.0095
2 ^b	0.0051	0.0084	1.0	0.0687	25245.62	2932714.78	0.0086	0.0066

6 (Assay: 99.0 %): d, 1.500 g/mL; FW, 120.38 g/mol. ^a Organic layer. ^b Water layer.

GC/MS analysis of reaction product solutions: GC reference spectra of CH₃OH solutions of 2, 3, 4, and 5.

CH₃OH (1.0 mL) solutions of commercially available **2**, **3**, **4**, and **5** (*ca.* 0.005 g) were prepared and then analysed by GC/MS spectroscopy (Figures S10, S11, S12, S13, respectively).

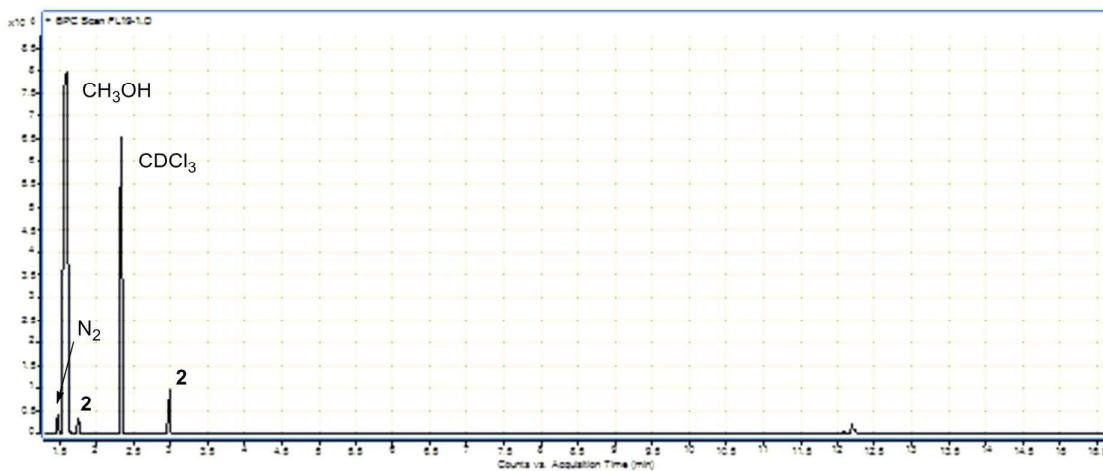


Figure S10. GC/MS spectrum of a CH₃OH solution of **2** (**2** generates, in the presence of CH₃OH, at the GC/MS experimental conditions, its hemiacetalic form.)

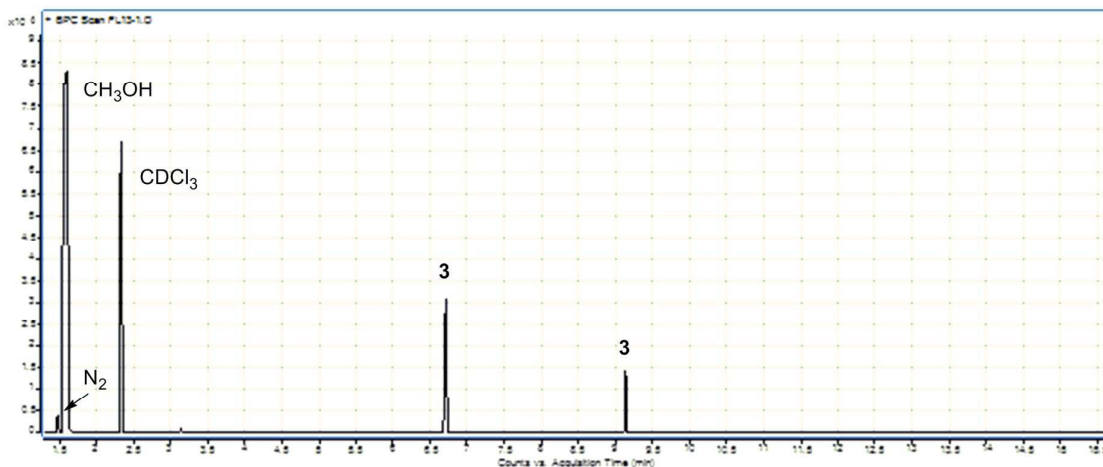


Figure S11. GC/MS spectrum of a CH₃OH solution of **3** (**3** generates, in the presence of CH₃OH, at the GC/MS experimental conditions, its hemiacetalic form.)

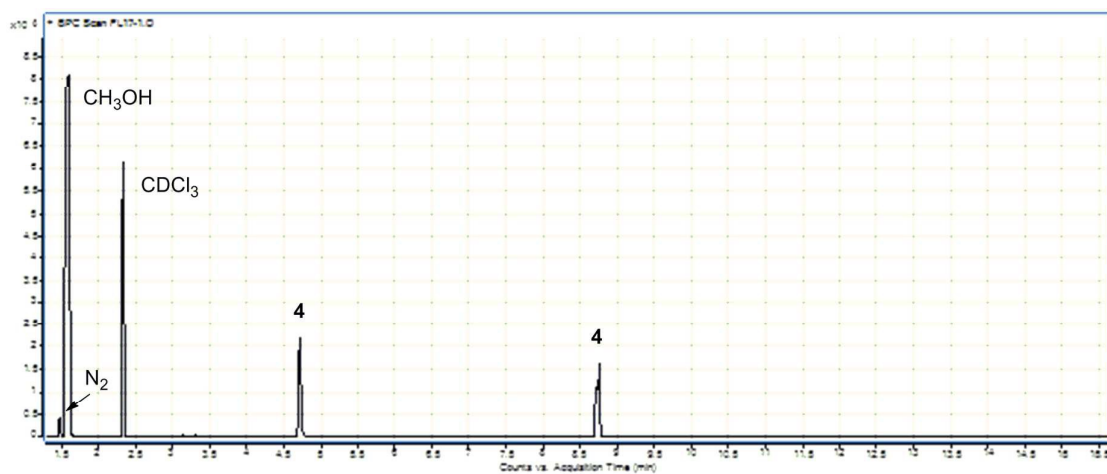


Figure S12. GC/MS spectrum of a CH₃OH solution of 4 (4 generates, in the presence of CH₃OH, at the GC/MS experimental conditions, its hemiacetalic form.)

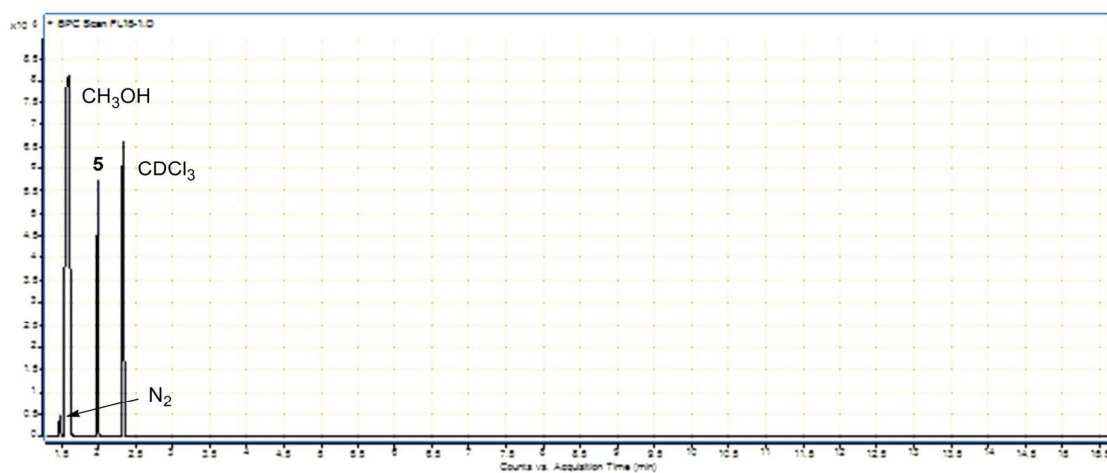


Figure S13. GC/MS spectrum of a CH₃OH solution of 5.

¹H NMR analysis of reaction product solutions.**¹H NMR analysis of reaction product solutions. General procedure.**

The collected reaction product solutions (*ca.* 0.010 g) were dissolved in CDCl₃ (*ca.* 0.7 mL). The following resonances of the four main components were investigated in the ¹H NMR spectrum of the resulting solutions: **5**, δ_{H} 3.60 (CH₂OH, t, $J_{\text{HH}} = 6.64$ Hz); **3**, δ_{H} 9.38 (C(O)H, s); **4**, δ_{H} 9.60 (C(O)H, d, $J_{\text{HH}} = 2.02$ Hz); **2**, δ_{H} 9.78 (C(O)H, m). The normalised ratio of the corresponding integrals (I₂, I₃, I₄, I₅ in tables S27, S28, S29, S30, S31, S32, S33, S34, S35) allowed calculating the molar ratio of **2**, **3**, **4**, and **5**.

Table S27. ¹H NMR analysis of the product solutions of HTID of 1,3-PDO in the presence of **1** and a base, in ionic liquids, and subsequent mass balance calculation: screening conditions experiments.

Entry	I ₅	n ₅ ^a [mol]	I ₂	n ₂ [mol]	I ₃	n ₃ [mol]	I ₄	n ₄ [mol]	MB ^b [%]
1	0.15	0.0009	1.00	0.0125	0.04	0.0005	0.01	0.0001	89
2	0.33	0.0007	1.00	0.0045	0.31	0.0014	0.11	0.0005	45
3	0.12	0.0002	1.00	0.0039	0.10	0.0004	0.11	0.0004	31
4	1.00	0.00002	1.00	0.00003	1.39	0.00005	0.00	0.0000	1
5	0.24	0.0012	1.00	0.0097	0.08	0.0008	0.04	0.0004	77
6	0.15	0.0005	1.00	0.0067	0.12	0.0008	0.06	0.0004	53
7	0.14	0.0006	1.00	0.0089	0.09	0.0008	0.05	0.0004	69
8	0.11	0.0001	1.00	0.0010	0.08	0.00008	0.05	0.00005	7
9	0.16	0.0005	1.00	0.0067	0.05	0.0003	0.03	0.0002	50
10	0.20	0.0012	1.00	0.0123	0.07	0.0009	0.03	0.0004	95
11	0.22	0.0002	1.00	0.0014	0.07	0.0001	0.08	0.0001	11
12	0.13	0.0006	1.00	0.0099	0.05	0.0005	0.02	0.0002	71
13	2.79	0.00004	1.00	0.00003	0.06	0.000002	0.00	0.0000	0.4
14	0.45	0.0006	1.00	0.0027	0.27	0.0007	0.13	0.0004	28
15	0.38	0.0004	1.00	0.0021	0.24	0.0005	0.14	0.0003	21
16	0.21	0.0002	1.00	0.0018	0.08	0.0001	0.02	0.00004	14
17	-	-	-	-	-	-	-	-	-
18	-	-	-	-	-	-	-	-	-
19	0.15	0.0007	1.00	0.0097	0.29	0.0028	0.13	0.0013	91
20	0.30	0.0011	1.00	0.0076	0.10	0.0008	0.03	0.0002	62
21	0.22	0.0010	1.00	0.0094	0.08	0.0008	0.07	0.0007	75
22	0.14	0.0008	1.00	0.0113	0.11	0.0012	0.06	0.0007	88
23	0.17	0.0006	1.00	0.0069	0.06	0.0004	0.15	0.0010	56
24	0.12	0.00001	1.00	0.0002	0.03	0.000006	0.22	0.00005	2
25	0.21	0.0009	1.00	0.0081	0.08	0.0006	0.03	0.0002	62
26	0.23	0.0010	1.00	0.0088	0.10	0.0009	0.05	0.0004	71
27	0.05	c	1.00	c	0.10	c	0.12	c	c
28	0.17	0.0007	1.00	0.0084	0.04	0.0003	0.01	0.0001	60
29	0.80	0.00003	1.00	0.00008	0.09	0.00001	0.66	0.0001	1
30	0.20	0.0012	1.00	0.0122	0.04	0.0005	0.02	0.0002	89
31	0.13	0.0030	1.00	0.0468	0.23	0.0108	0.10	0.0047	403 ^d
32	0.19	0.0024	1.00	0.0248	0.16	0.0040	0.08	0.0020	205 ^d

^a n₅ was calculated *via* GC/MS analysis of the product solutions. ^b MB = Mass balance. ^c The intensity of the GC peak due to **5** was so little that no reliable integration could be obtained and so no reliable mass balance calculations could be achieved. ^d In entries 31 and 32, 1,3-PDO was used as both the substrate and the solvent.

Table S28. ^1H NMR analysis of the product solutions of HTID of 1,3-PDO in the presence of **1** and K_2CO_3 , in EmmimNTf_2 , at T 150 °C, and at $[\text{1,3-PDO}]:[\text{Ir}] \cong 75.0$, and subsequent mass balance calculations: recycling experiments.

Entry	I_5	n_5^a [mol]	I_2	n_2 [mol]	I_3	n_3 [mol]	I_4	n_4 [mol]	MB ^b [%]
1	0.30	0.0015	1.00	0.0098	0.09	0.0009	0.05	0.0005	78
2	0.72	0.0037	1.00	0.0104	0.05	0.0005	0.00	0.0000	91
3	0.64	0.0025	1.00	0.0077	0.04	0.0003	0.00	0.0000	64
4	0.79	0.0042	1.00	0.0105	0.05	0.0005	0.00	0.0000	95
5	0.84	0.0040	1.00	0.0095	0.04	0.0004	0.00	0.0000	86
6	0.85	0.0037	1.00	0.0086	0.05	0.0004	0.00	0.0000	79
7	0.78	0.0038	1.00	0.0097	0.04	0.0004	0.00	0.0000	86
8	0.86	0.0028	1.00	0.0066	0.05	0.0003	0.00	0.0000	61
9	0.83	0.0031	1.00	0.0074	0.05	0.0004	0.00	0.0000	68
10	0.79	0.0028	1.00	0.0070	0.05	0.0004	0.00	0.0000	62

^a n_5 was calculated *via* GC/MS analysis of the product solutions. ^b MB = Mass balance.

Table S29. ^1H NMR analysis of the product solutions of HTID of 1,3-PDO in the presence of **1** and K_2CO_3 , in $\text{N}_{1,8,8}\text{NTf}_2$, at T 150 °C, and at $[\text{1,3-PDO}]:[\text{Ir}] \cong 75.0$, and subsequent mass balance calculations: recycling experiments.

Entry	I_5	n_5^a [mol]	I_2	n_2 [mol]	I_3	n_3 [mol]	I_4	n_4 [mol]	MB ^b [%]
1	0.14	0.0006	1.00	0.0086	0.04	0.0003	0.03	0.0003	61
2	0.40	0.0006	1.00	0.0028	0.03	0.0001	0.01	0.00003	21
3	0.29	0.0011	1.00	0.0076	0.06	0.0005	0.02	0.0002	58
4	0.33	0.0017	1.00	0.0104	0.07	0.0007	0.02	0.0002	81
5	0.36	0.0014	1.00	0.0081	0.06	0.0005	0.01	0.0001	63
6	0.24	0.0013	1.00	0.0106	0.06	0.0006	0.02	0.0002	79
7	0.36	0.0016	1.00	0.0087	0.06	0.0005	0.02	0.0002	68
8	0.28	0.0014	1.00	0.0103	0.09	0.0009	0.04	0.0004	81
9	0.24	0.0015	1.00	0.0127	0.08	0.0010	0.03	0.0004	98
10	0.37	0.0012	1.00	0.0065	0.07	0.0005	0.03	0.0002	52

^a n_5 was calculated *via* GC/MS analysis of the product solutions. ^b MB = Mass balance.

Table S30. ^1H NMR analysis of the product solutions of HTID of 1,3-PDO in the presence of **1** and K_2CO_3 , in EmmimNTf_2 , at T 150 °C, and at $[\text{1,3-PDO}]:[\text{Ir}] \cong 220.0$, and subsequent mass balance calculations: recycling experiments.

Entry	I_5	n_5^a [mol]	I_2	n_2 [mol]	I_3	n_3 [mol]	I_4	n_4 [mol]	MB ^b [%]
1	0.16	0.0010	1.00	0.0131	0.07	0.0009	0.05	0.0007	98
2	0.39	0.0015	1.00	0.0078	0.07	0.0005	0.00	0.0000	62
3	0.38	0.0013	1.00	0.0068	0.12	0.0008	0.01	0.0001	56
4	0.32	0.0015	1.00	0.0094	0.06	0.0006	0.00	0.0000	72
5	0.37	0.0015	1.00	0.0078	0.07	0.0005	0.00	0.0000	61

^a n_5 was calculated *via* GC/MS analysis of the product solutions. ^b MB = Mass balance.

Table S31. ^1H NMR analysis of the product solutions of HTID of 1,3-PDO in the presence of **1** and K_2CO_3 , in $\text{N}_{1,8,8,8}\text{NTf}_2$, at T 150 °C, and at $[\text{1,3-PDO}]:[\text{Ir}] \cong 220.0$, and subsequent mass balance calculations: recycling experiments.

Entry	I_5	n_5^a [mol]	I_2	n_2 [mol]	I_3	n_3 [mol]	I_4	n_4 [mol]	MB ^b [%]
1	0.11	0.0006	1.00	0.0100	0.03	0.0003	0.02	0.0002	69
2	0.25	0.0008	1.00	0.0067	0.07	0.0005	0.01	0.0001	50
3	0.24	0.0011	1.00	0.0094	0.08	0.0007	0.01	0.0001	70
4	0.29	0.0012	1.00	0.0082	0.08	0.0007	0.01	0.0001	63
5	0.22	0.0009	1.00	0.0081	0.05	0.0004	0.01	0.0001	59

^a n_5 was calculated *via* GC/MS analysis of the product solutions. ^b MB = Mass balance.

Table S32. ^1H NMR analysis of the product solutions of HTID of 1,3-PDO in the presence of **1** and K_2CO_3 , in EmmimNTf_2 , at T 120 °C, and at $[\text{1,3-PDO}]:[\text{Ir}] \cong 75.0$, and subsequent mass balance calculations: recycling experiments.

Entry	I_5	n_5^a [mol]	I_2	n_2 [mol]	I_3	n_3 [mol]	I_4	n_4 [mol]	MB ^b [%]
1	0.12	0.0007	1.00	0.0115	0.11	0.0013	0.09	0.0010	90
2	0.16	0.0008	1.00	0.0103	0.09	0.0009	0.05	0.0005	79
3	0.21	0.0011	1.00	0.0108	0.12	0.0013	0.02	0.0002	84
4	0.24	0.0012	1.00	0.0096	0.10	0.0010	0.02	0.0002	75
5	0.27	0.0014	1.00	0.0101	0.09	0.0009	0.01	0.0001	78

^a n_5 was calculated *via* GC/MS analysis of the product solutions. ^b MB = Mass balance.

Table S33. ^1H NMR analysis of the product solutions of HTID of 1,3-PDO in the presence of **1** and K_2CO_3 , in $\text{N}_{1,8,8,8}\text{NTf}_2$, at T 120 °C, and at $[\text{1,3-PDO}]:[\text{Ir}] \cong 75.0$, and subsequent mass balance calculations: recycling experiments.

Entry	I_5	n_5^a [mol]	I_2	n_2 [mol]	I_3	n_3 [mol]	I_4	n_4 [mol]	MB ^b [%]
1	0.08	0.0005	1.00	0.0116	0.12	0.0014	0.07	0.0008	89
2	0.31	0.0009	1.00	0.0061	0.11	0.0007	0.04	0.0002	50
3	0.29	0.0014	1.00	0.0097	0.08	0.0008	0.01	0.0001	74
4	0.36	0.0011	1.00	0.0063	0.06	0.0004	0.03	0.0002	50
5	0.38	0.0015	1.00	0.0081	0.05	0.0004	0.02	0.0002	64

^a n_5 was calculated *via* GC/MS analysis of the product solutions. ^b MB = Mass balance.

Table S34. ^1H NMR analysis of the product solutions of mercury poisoning test of the iridium precatalyst in HTID of 1,3-PDO in the presence of **1** and K_2CO_3 , in EmmimNTf_2 , and subsequent mass balance calculations.

I_5	n_5^a [mol]	I_2	n_2 [mol]	I_3	n_3 [mol]	I_4	n_4 [mol]	MB ^b [%]
0.15	0.0008	1.00	0.0101	0.07	0.0007	0.05	0.0005	75

^a n_5 was calculated *via* GC/MS analysis of the product solutions. ^b MB = Mass balance.

Table S35. ^1H NMR analysis of the product solutions of HTID of 1,3-PDO in the presence of **1** and K_2CO_3 , at 120 °C, in EmmimNTf_2 and $\text{N}_{1,8,8,8}\text{NTf}_2$, and water, at $[\text{1,3-PDO}]:[\text{Ir}] \cong 75.0$, and subsequent mass balance calculations.

Entry	I_5	n_5^a [mol]	I_2	n_2 [mol]	I_3	n_3 [mol]	I_4	n_4 [mol]	MB ^b [%]
1	0.25	0.0015	1.00	0.0123	0.04	0.0005	0.00	0.0000	88
2 ^c	0.45	0.0005	1.00	0.0021	0.41	0.0008	0.19	0.0004	23
2 ^d	0.51	0.0002	1.00	0.0007	0.05	0.00004	0.01	0.00001	6

^a n_5 was calculated *via* GC/MS analysis of the product solutions. ^b MB = Mass balance. ^c Organic layer. ^d Water layer.

HTID of 1,3-PDO in the presence of **1 and K_2CO_3 , in $N_{1,8,8,8}NTf_2$, at T 150 °C, and at [1,3-PDO]:[Ir] \cong 220.0: monitoring potential decomposition of ionic liquids and **1**.**

1,3-PDO (in Table S36, see 1,3-PDO in entry 1), **1** (in Table S36, see **1** in entry 1), K_2CO_3 (in Table S36, see K_2CO_3 in entry 1), and $N_{1,8,8,8}NTf_2$ (in Table S36, see $N_{1,8,8,8}NTf_2$) were mixed in a 50 mL round bottom flask connected, through a distillation condenser, to a 50 mL glass tube. The mixture was reacted at 150 °C, at a controlled pressure of *ca.* 0.35 bar, for 1 hour, stirring at 1000 rpm. The reaction product, a colourless liquid, was isolated by distillation, being collected, for the duration of the 1 hour reaction, in the collecting glass tube kept at *ca.* -196 °C (N_2 (l) bath). The reacted mixture, left in the 50 mL round bottom flask, was analysed by 1H NMR spectroscopy. The reaction was repeated reacting 1,3-PDO, **1**, K_2CO_3 , and $N_{1,8,8,8}NTf_2$ for 2 (Table S36, entry 2), 3 (Table S36, entry 3), 4 (Table S36, entry 4), 5 (Table S36, entry 5), and 6 (Table S36, entry 6) hours. The reacted mixture, left in the 50 mL round bottom flask in each of such reactions, was analysed by 1H NMR spectroscopy.

HTID of 1,3-PDO in the presence of **1 and K_2CO_3 , in $EmmimNTf_2$ and $N_{1,8,8,8}NTf_2$, at T 150 °C, and at [1,3-PDO]:[Ir] \cong 75.0: monitoring iridium hydride complexes formation.**

1,3-PDO (in $EmmimNTf_2$: 0.1245 g, 0.0016 mol; in $N_{1,8,8,8}NTf_2$: 0.1257 g, 0.0016 mol), **1** (in $EmmimNTf_2$: 0.0120 g, 0.021 mmol; in $N_{1,8,8,8}NTf_2$: 0.0112 g, 0.020 mmol), K_2CO_3 (in $EmmimNTf_2$: 0.0068 g, 0.049 mmol; in $N_{1,8,8,8}NTf_2$: 0.0069 g, 0.050 mmol), and $EmmimNTf_2$ (0.2789 g, 0.688 mmol) or $N_{1,8,8,8}NTf_2$ (0.4510 g, 0.695 mmol) were mixed in a 50 mL round bottom flask connected, through a distillation condenser, to a 50 mL glass tube. The mixture was reacted at 150 °C, at a controlled pressure of *ca.* 0.35 bar, for 3 hours, stirring at 1000 rpm. The reaction product, a colourless liquid, was isolated by distillation, being collected, for the duration of the 3 hours reaction, in the collecting glass tube kept at *ca.* -196 °C (N_2 (l) bath). The reacted mixture, left in the 50 mL round bottom flask, was analysed by 1H NMR spectroscopy.

Table S36. HTID of 1,3-PDO in the presence of **1** and K₂CO₃, in N_{1,8,8,8}NTf₂, at T 150 °C, and at [1,3-PDO]:[Ir] ≅ 220.0: experimental data for experiments on monitoring potential decomposition of ionic liquids and **1**.

Entry	1,3-PDO [g]	n(1,3-PDO) [mol]	1 [g]	n(1) [mmol]	K ₂ CO ₃ [g]	n(K ₂ CO ₃) [mmol]	N _{1,8,8,8} NTf ₂ [g]	n(N _{1,8,8,8} NTf ₂) [mol]
1	0.1244	0.0016	0.0115	0.020	0.0064	0.046	0.4615	0.0007
2	0.1245	0.0016	0.0124	0.022	0.0062	0.045	0.4750	0.0007
3	0.1209	0.0016	0.0119	0.021	0.0063	0.045	0.4650	0.0007
4	0.1223	0.0016	0.0112	0.020	0.0068	0.049	0.4623	0.0007
5	0.1152	0.0015	0.0112	0.020	0.0069	0.050	0.4781	0.0007
6	0.1205	0.0016	0.0121	0.021	0.0066	0.048	0.4633	0.0007

All operations were carried out (a) at P = 0.35 bar; (b) at RPM: 1000.

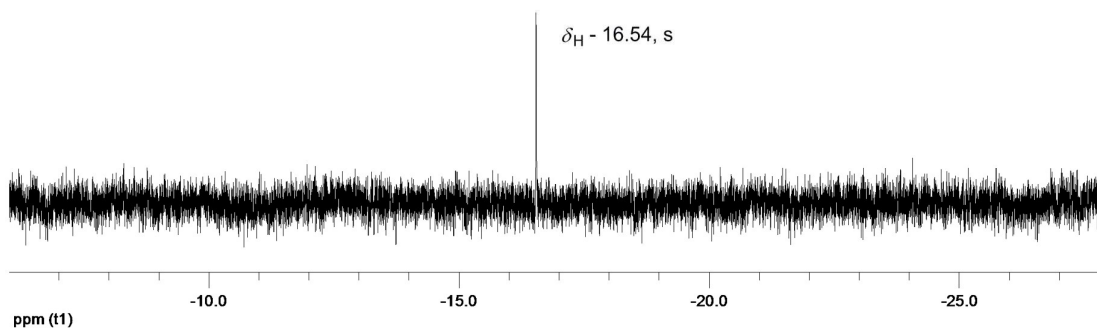


Figure S14. ^1H NMR spectrum of the reacting mixture of HTID of 1,3-PDO in the presence of **1** and K_2CO_3 , in $\text{N}_{1,8,8,8}\text{NTf}_2$, at $150\text{ }^\circ\text{C}$, and at a dynamic vacuum of *ca.* 0.35 bar: enlargement of the hydride region ($\delta_{\text{H}} - 6.00 - \delta_{\text{H}} - 28.00$).

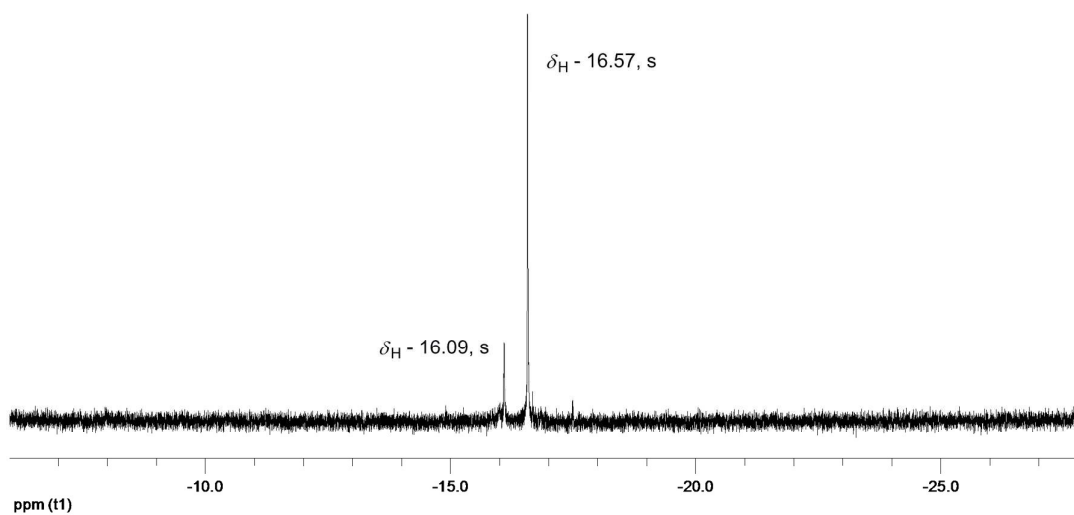


Figure S15. ^1H NMR spectrum of the reacting mixture of HTID of 1,3-PDO in the presence of **1** and K_2CO_3 , in EmmimNTf_2 , at $150\text{ }^\circ\text{C}$, and at a dynamic vacuum of *ca.* 0.35 bar: enlargement of the hydride region ($\delta_{\text{H}} - 6.00 - \delta_{\text{H}} - 28.00$).



Figure S16. Experimental apparatus for the HTID of 1,3-PDO in the presence of **1** and a base, in ionic liquids, towards selective production of propionaldehyde.